EFFECTS OF HILLS ON SURFACE WAVES

A DISSERTATION

Submitted in partial fulfillment of the requirements for the award of the degree

of

MASTER OF TECHNOLOGY

in

EARTHQUAKE ENGINEERING

(With Specialization in Seismic Vulnerability and Risk Assessment)

By

RANU CHAUHAN

(14553008)

Under the Guidance of

Dr. J.P. NARAYAN

DEPARTMENT OF EARTHQUAKE ENGINEERING

INDIAN INSTITUTE OF TECHNOLOGY ROORKEE

ROORKEE – 247667

MAY 2016

CANDIDATE'S DECLARATION

I Ranu Chauhan, hereby declare that the thesis work, which is being presented in this dissertation entitled**, " Effects of hills on Surface Waves ",** in the partial fulfillment of the requirements for the award of the degree of **Master of Technology** in **Earthquake Engineering**, with specialization in **Seismic Vulnerability & Risk Assessment**, submitted in the Department of Earthquake Engineering, Indian Institute of Technology Roorkee, is an authentic record of my own work carried out for a period from June 2015 to May 2016 under the guidance of **Dr. J.P. NARAYAN**, Professor, Department of Earthquake Engineering, Indian Institute of Technology Roorkee, Roorkee.

The matter embodied in this report has not been submitted by me for the award of any other degree or diploma of this Institute or any other University/Institute**.**

RANU CHAUHAN
(14553008)
M.Tech (2^{nd} year) SVRA
Department of Earthquake Engineering
I.I.T.Roorkee

Place: Roorkee
Date: MAY, 2016

CERTIFICATE

This is to certify that the above statement made by the candidate is correct to the best of my knowledge.

Dr. J.P. Narayan
Professor
Department of Earthquake Engineering
I.I.T Roorkee

Place: Roorkee
Date: MAY, 2016

ACKNOWLEDGEMENT

The success of this project depends largely on my guide Dr. J. P. Narayan, Professor, Department of Earthquake Engineering, I.I.T Roorkee. I have been really fortunate to have him as my guide and mentor and would like to show my greatest gratitude to him for his tremendous support and help. Without his encouragement and guidance this dissertation would not have materialized.

The encouragement and guidance of many others has also been a great help and motivation all throughout the completion. I take this opportunity to express my gratitude to my family, my dear friends and all the people who have been instrumental in the successful completion of this seminar.

RANU CHAUHAN

(14553008)

M.Tech (2^{nd} year) SVRA

Department of Earthquake Engineering

I.I.T Roorkee

Place: Roorkee

Date: MAY, 2016

ABSTRACT

We have studied the effect of topography including ridge and valley on Rayleigh wave characteristics. A fourth order finite difference method is used for simulations. Gabor wavelet is used as a source time function. We have computed the seismic response of ridge and valley with different shape ratio and also by changing the geometry of the topography. Based on the analysis of simulated results, it is observed that ridge amplify the horizontal component and de-amplify the vertical component at the crest whereas valley de-amplify both the horizontal and vertical component. Amplification of horizontal component increases with increase in shape ratio and also the rate of de-amplification in case of vertical component increases with increase in shape ratio. Secondly, we have observed that after the complex interaction of Rayleigh wave with the topography splitting of the wave occurs and there is time separation between the two splits. One of the split of Rayleigh wave remain unaffected by the topography and the other passes through the flanks of the topography. This time separation increases with increase in the shape ratio.

We have also analysed the seismic responses of combinations of various ridge and valley together. It can be concluded that if Rayleigh wave first interact with the valley rather than the ridge than the de-amplification occurs and the energy remained in the signal at the last stations is very negligible. Generally the amplitude of high frequency signal is nearly zero hence the valley act as a sinking zone for high frequency waves. These combinations are analysed so that we can relate the hazard associated with it and can recommend the safe location for building up the houses avoiding landslides, etc.

TABLE OF CONTENTS

LIST OF FIGURES

LIST OF TABLES

INTRODUCTION

Today one of the most important issues about the structural damages caused by earthquake is the evaluating of the spectral response of the site on which the construction is built. Various field observations revealed that loose soil cover (Rann area), liquefaction, heavily alleviated low land regions and topographical features like ridge and valley have played asignificant role in damage.It is seen that lesser intensities were observed in the hard rock areas, while higher intensities were observed on the alluvium soil cover. It was concluded on the basis of the observation that local geology rather than engineering features of structures largely determined the severity of damage during the earthquake. According to studies, features of the site materials and geometry of the ground surface are considered as the main factors.

From the past study it was noticed that even a small magnitude can cause large devastation in hilly region so there arise a need of studying the topography effects on surface waves.As we know that surface waves are generally more damaging than body waves because they are much closer to the buildings and can cause large differential motion to the foundation of buildings due to differences in travel path.Earlier studies shows that surface waves mainly Rayleigh wave is strongly affected by the surface irregularities like ridge and valley, etc. when wavelength of wave is comparable to width of the topography.It basically affect on its wave form, frequency characters and propagation energy, especially for high frequency part. In order to apply surface waves to theoretical and practical seismic problem it is necessary to study such topographic effect. Study of topography effect began with the study of reflection and transmission coefficient of Rayleigh wave. Hence in hazard prediction the surface wave has very important role.

Main reason of this fact is the amplification/de-amplification of seismic waves after interaction with the topographical features like ridges and valleys. It has been seen that the crest of ridge or the top of mountain amplify P, SV and Rayleigh wave amplitudes

(Sanchez-Sesma et al., 1992). The amplification of ground motion has been observed and studied for some past earthquakes like 1985 chile earthquake (Celebi and Hanks,1986) and the 1999 Athens,Greece earthquake (Assimaki et al, 2005). Effect of large scale topography on ground motion generated by nearby fault is also interesting area of study. Large scale topography acts as a natural seismic insulator for the area which is situated opposite side of the epicentre of earthquake.

1.1 LITERATURE REVIEW

Wong (1982) studied the diffraction of P, SV and Rayleigh wave at the vicinity of a semi-elliptical canyon. He concluded that high frequencies of Rayleigh wave could not pass the canyon.Francisco et al (1991)studied the diffraction of P, SV and Rayleigh waves by topographical features. The conclusion was that the amplification due to topography was less than four time of the amplitude of incident wave.

Savage (2004) used the analytical solution of topography models using free Rayleigh wave propagation across isolated symmetrical ridges and valleys. He concluded that horizontal component of Rayleigh wave gets amplified at ridge crest when wavelength of Rayleigh wave are comparable to the ridge width and the same gets strongly de-amplified at the valley bottom when Rayleigh wavelength is comparable to valley width. Cherry (1973) explained the reason behind the landslides in case of unstable slopes is retrograde motion of Rayleigh wave.

Zhou, H,Chen (2007) studied the response of irregular topography on combination of P-wave and Rayleigh wave generated with an explosive source and concluded that steeper topography block more Rayleigh waves having high frequency content. Irregular topography not only changes the energy content but also the frequency response and also various wave conversions happens.Shou et al. (2007)examined the effect of large scale topography on ground motion using the combined seismic response of San Gabriel Mountains and Los Angeles basin, California and concluded that large mountains surrounding basin act as a natural seismic insulator by scattering of the surface waves and hence leads to less- efficient excitation of basin.

1.2 OBJECTIVE OF THE WORK

The extensive literature review revealed that there are many researchers who studied the effect of topography on body wave characteristics. But, there arelimited number of researchers who studied the effect of topography on the characteristics surface waves. The main reason behind this is that the most of earthquake records does not contain surface waves.The amplification is studied with respect to various frequencies which is helpful in construction of structure. Further, such study is also useful in microzonation of hilly areas. In this work, the effect of ridge and valley of different shapes and their combinations on characteristics of Rayleigh waves is studied in details.

1.3 LAYOUT OF THE THESIS

In chapter 1, a brief idea about the work done in the past by various researchers on effect of topography on surface waves and body waves and objective of our work is presented. In chapter 2, introduced the finite difference method used in my thesis and various stability conditions to be used in analysis work. In chapter 3, topographic models, grid size, unrelaxed parameters, anelastic parameters are defined and also showed the effect of shape ratio on Rayleigh wave which is intern generated using shear stress in the form of Gabor wavelet and also conclude the time separation before and after passing the topography. In chapter 4, effect of combination of ridge-valley topography on various characteristics of Rayleigh wave is studies after analyzing the amplitude, spectral amplitude and spectral ratio at various key locations. In chapter 5, various conclusions drawn based on numerical analysis of response of ridge and valley models and their combinations.

Chapter # 2

DESCRITIZATION OF RIDGE AND VALLEY MODEL USING FINITE DIFFERENCE METHOD

2.1 INTRODUCTION

Finite difference method is one of the most important numerical method in seismology and a dominant method in earthquake ground motion modeling. Formally, it is applicable to complex models, relatively accurate and computationally efficient. FDM is also called grid-point method. In this method a computational domain is covered by space- time grid and each function is represented by its values at grid points. Space-time distribution significantly affects the accuracy of approximation. It helps in simulating the various waves like P, P-SV, SH and Rayleigh waves.

Various steps used in this method are as follows:

- Descritise the space-time model using particular grid size and time step based on consistency, stability, convergence and grid dispersion conditions.
- Assign the parameters to each grid point as per staggering technique.
- Source is inserted into numerical grid at desired location in the form of stress.
- Particle velocity is computed at each node at updated time 'n+1'.

In this thesis, a P-SV wave staggered-grid, fourth order accurate viscoelastic FD program developed by Narayan and Kumar (2014) is used to simulate the responses of the considered topography models. There is two type of FD approximation of P-SV wave equation in staggered grid. For these approximations, two types of operators are being used. These operators are developed using Taylor's series expansion. The operators as well as approximations are second order (2,2) and fourth order (2,4) type for the temporal and the spatial discretisation.We have used forth order approximation because it gives better

result with good accuracy than second order approximation.FD scheme should be consistent with the original problem, stable and convergent.

2.2 FREE SURFACE BOUNDARY CONDITION

It is important to implement the boundary conditions at the free surface for greater accuracy of FD method. There are two types of free surface boundary conditions:

i.**Vacuum formulation**(Boore, 1972; Randaall 1989): In this the values of elastic parameters are set to zero and density is reduced marginally above the free surface. This approach is attractive because it can be implemented with the same finite difference equation are used in interior of model. It gives good accuracy in the displacement formulation.

ii. **Stress imaging technique**(Lavander 1988; graves 1996): In this method explicit boundary conditions are applied to the stress tensor components located at the grid plane coinciding with the free surface. Moreover, anti-symmetry of the stress tensor components with respect to the free surface is assumed.We are using vacuum formulation in our FD Method.

2.3 ABSORBING BOUNDARY CONDITION

Because of limited available computer memory, the numerical models have certain fixed dimensions. The waves travelling through the grid of model are reflected back from the model edges, known as **edge- reflections** . To avoid these reflections absorbing boundary conditions are applied along the edge of the model. These conditions are divided into two groups:

i. The first group, including the popular Clayton and Engquist(1977), attempt to extrapolate the wavefield beyond the edge of the computational domain and then use this extrapolate wavefield to update the interior grid points.

ii. The second group, including the approach of Israeli and Orszag(1981), gradually attenuate the amplitude of wavefield within a ‘sponge layer’.

2.4 STABILITY CONDITION

Stability condition for P-wave, SH- wave and P-SV wave FD simulation with second order special accuracy is

$$\frac{V_{MAX}\,\Delta t}{\text{Min}(\Delta x \text{ or } \Delta z)} \leq \frac{1}{\sqrt{2}}$$

The stabilitycondition for P-wave, SH- wave and P-SV wave FD simulation with forth order specialaccuracy :

$$\frac{V_{MAX}\,\Delta t}{\text{Min}(\Delta x \text{ or } \Delta z)} \leq \frac{6}{7\sqrt{2}}$$

Grid-dispersion relation is relation between grid velocity, special grid spacing, time step and material properties, obtained from the stability condition. Atleast 10 grid spacings should be used to sample the wavelength λ in order to avoid grid dispersion of the phase and group velocities for the wavelength λ in second order approximation and five or six grid spacing per wavelength in fourth order approximation. It is more important in viscoelastic media than in case of elastic media.

The P-SV wave FD program of Nrarayan and Kumar (2014) is based on the staggered grid second-order accurate in time and fourth-order accurate in space(2,4) FD approximation of the viscoelastic P-SV wave equations for the heterogeneous anelastic medium with a variable grid size. The frequency-dependent damping in the time domain FD simulations is incorporated based on GMB-EK rheological model (Emmerich and Korn, 1987). A material independent anelastic function developed by Kristek andMoczo (2003) are used since it is preferable in case of material discontinuities in the FD grid.

An improved vacuum formulation proposed by Zeng et al. (2012) is used as free surface boundary condition. Both the sponge boundary (ISsraeli and Orszag, 1981) and A1 absorbing boundary (Clayton and Engquist, 1977) conditions were implemented on the model edges to avoid the edge reflections (Kumar and Narayan, 2008).

2.5 SOURCE EXCITATION FUNCTION

The important property of the wavelet is that it minimizes the product of its standard deviations in the time and frequency domain. Put another way, the uncertainty in information carried by this wavelet is minimized. However they have the downside of being non-orthogonal, so efficient decomposition into the basis is difficult. The equation for Gabor wavelet is the mathematical relation for generating the Gabor is

$$S(t) = Exp(-\alpha)cos[\omega_P(t - t_S) + \varphi]$$

Where$\alpha = \left[\frac{\omega_P(t-t_S)}{\gamma}\right]^2$, fp is predominant frequency, γ controls the oscillatory character, $t_S$controlsthe duration (duration=2t_S) and φ is phase shift.

As opposed to other functions commonly used as bases in Fourier Transforms such as sine and cosine, Gabor wavelets have locality properties, meaning that as the distance from the center increases, the value of the function becomes exponentially suppressed.

The shear stress in the form of Gabor pulse is applied at the source location in FD grid to generate the P- and SV-wave. If only shear stress is applied then the amplitude of generated P-wave is negligible as compared to the amplitude of the SV-wave. Figure shown below shows the generatedGabor pulsefor fp=4,γ= 0.25, t_S=1.5 and φ=0 and itsspectra.

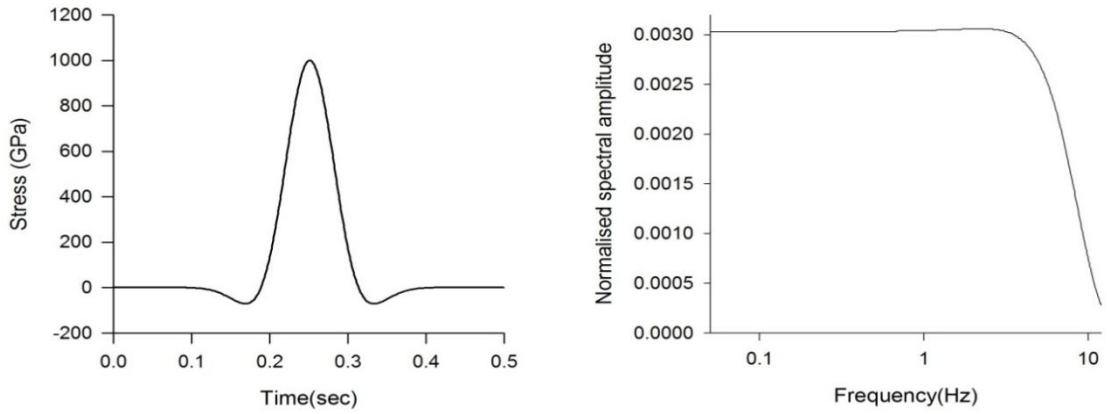

Figure 2.1 Gabor wavelet and its normalized spectra

Chapter#3

ANALYSIS OF SEISMIC RESPONSES OF RIDGE VALLEY MODELS AND THE EFFECT OF SHAPE RATIO

3.1 DISCRETISATION OF MODELS AND INPUT PARAMETERS

To insert the ridge and valley models into the FD numerical grid, we need to know the grid size by satisfying the stability conditions given for fourth order approximation in homogeneous medium (Moczo et al., 2000). Another condition which should be satisfied is grid dispersion. As we know that grid size should be equal to one-sixth of the shortest wavelength of interest in the fourth order FD approximation.

$V=f*\lambda$

V= velocity of S-wave

f =highest frequency in the frequency band

λ= shorted wavelength of S-wave

From the above formula calculated minimum grid size is 3m and maximum grid size is 10m.

Minimum size of grid depends upon two reasons:

- To avoid grid dispersion
- To make smooth boundary of model

We have taken uniform grid size of 3m in X-direction which led to total number of grids in X-direction is 3000. Absorbing boundary conditions (dampers) are applied from 0-200 grids and then from 2200-2400. In between these two dampers there lies main model.Varying grid size is taken in Z-direction as 3m from 1-300 grids and 10m from 300-1000 grids leads to total 1000 grids in Z-direction.Free surface is taken at 200 grid point from top in ridge models and at 10 grid point in valley models. Above that there is air and below there is rock. Density of air is assumed one-tenth of density of rock.

Rayleigh wave have been generated by using shear stress in the form of Gabor wavelet at a depth of 100m below the free surface. Gabor wavelet of dominant frequency 4Hz is considered to see the effect of topography on Rayleigh wave generated. For this frequency

band is from 0-12 Hz.A point source in inserted into the numerical grid at a distance of 660 m and at a depth of 100 m. The time step is taken as 0.001 sec to avoid the stability problem.Tables 3.1, 3.2 and 3.3 shows the discretisation of ridge and valley models.

Table 3.1 Grid size in X direction.

Material	X-direction		
	Grid	Grid size (m)	Total length(m)
Damper	1-200	3	600
Rock	200-2200	3	6000
Damper	2200-2400	3	600

Table 3.2 Grid size in Z-direction in case of Ridge models.

Material	Z-direction		
	Grids	Grid size(m)	Total length (m)
Air	1-200	3	450
Rock	200-300	3	450
Rock	300-800	10	5000
Damper	800-1000	10	2000

Table 3.3 Grid size in Z-direction in case of Valley models:

Material	Z-direction		
	Grids	Grid size(m)	Total length (m)
Air	1-10	3	30
Rock	10-300	3	870
Rock	300-800	10	5000
Damper	800-1000	10	2000

The value of P- and S-wave velocities, quality factors a reference frequency (F_r=1), density and Poisson's ratio for the homogeneous visco-elastic medium have been given in table 3.4. Quality factor is taken as 10 % of S-wave velocity.

Table 3.4 Parameters for homogenous visco-elastic material

Material	Density (kg/m^3)	V_S(m/s)	V_P (m/s)	Q_s	Q_p	Poisson's Ratio (ν)
Rock	2200	1000	1700	100	170	0.25

The unrelaxed moduli and the anelastic coefficients for both the shear modulus and the bulk modulus have been calculated at four relaxation frequencies of 0.02, 0.2, 2, 20 Hz and given in table 3.5

Table 3.5 Computed input parameters

Material	Unrelaxedmodulai			Anelastic coefficient		
	μ_u(Gpa)	K_U(Gpa)	λ_U(Gpa)	Y_α (I=1,4)	Y_β (I=1,4)	Y_Υ (I=1,4)
Rock	2.222	6.345	1.9	0.009686	0.015988	-0.00505241
				0.008262	0.013802	-0.00469433
				0.008348	0.014047	-0.00498018
				0.010134	0.017264	-0.00654084

The seismic response of the model containing source and the topography has been computed at 32equidistant receiver points (60 m apart) extending from 360 m epicentral distance to 5760 m.

3.2 SEISMIC RESPONSE OF HOMOGENEOUS MODEL

In order to infer the effects of topography on the characteristics of the Rayleigh, the response of the model with or without topography are compared and analysed. Figure 3.2 shows the homogeneous model named HOMO Model.

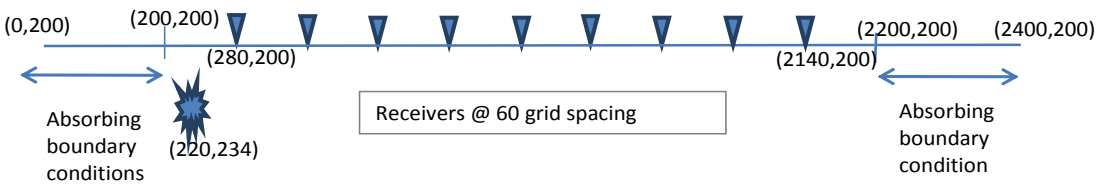

Figure 3.1HOMO Model

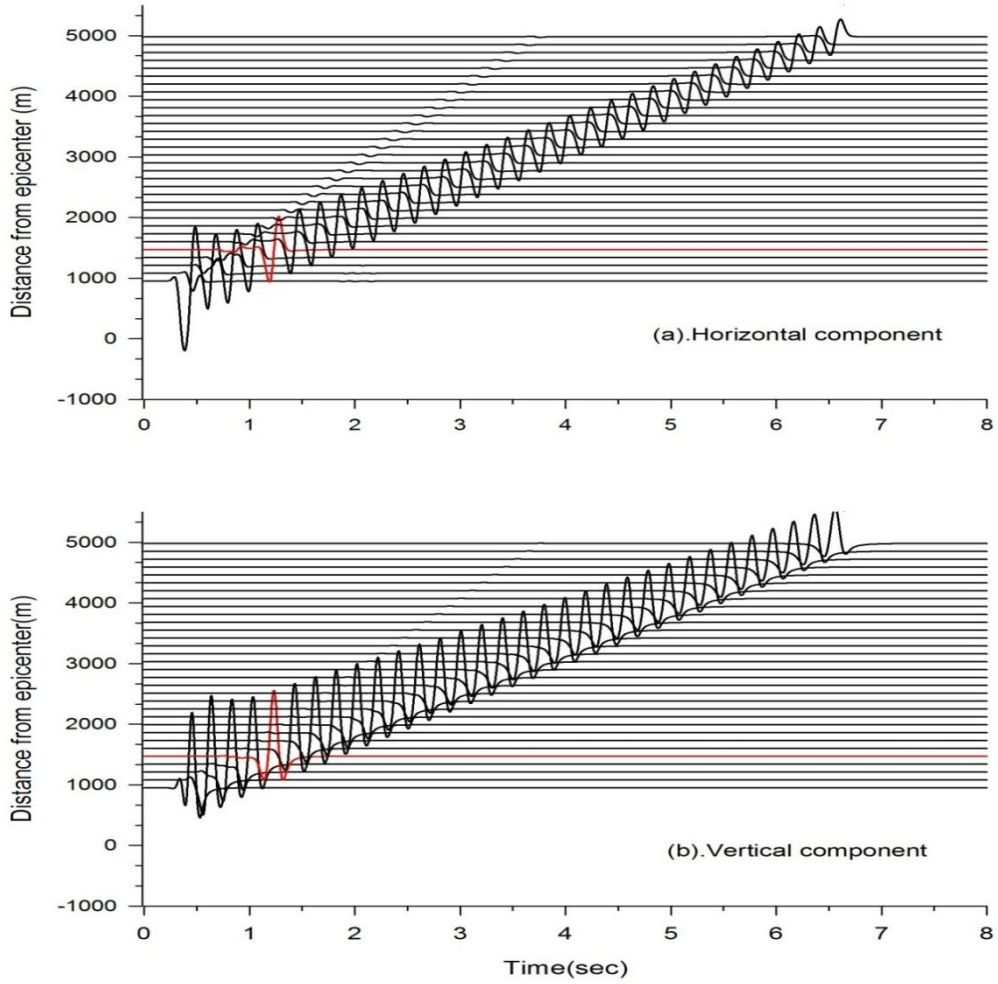

Fig.3.2 Horizontal and vertical components of particle velocity response of HOMO Model

Analysis of figure 3.2 reveals that the amplitude of vertical component is larger to that in the vertical component, which is obvious one in the homogeneous medium. The is minor decrease of amplitude of Rayleigh wave with distance travelled due to viscoelastic damping only since there is no divergence effect on the Rayleigh wave.

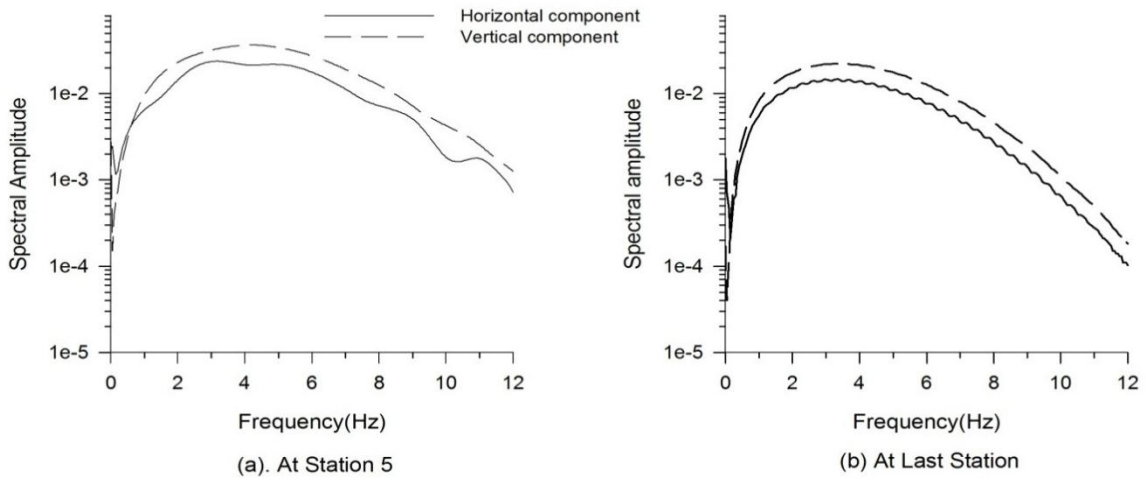

Fig.3.3 Spectral amplitudes of horizontal and vertical components at two locations in HOMO Model.

The analysis of figure 3.3 very clearly shows that the spectral amplitudes in the horizontal components are lesser than that in the vertical component. Spectral amplitude is computed at station 5 which is the location where crest of the ridge and bottom of the valley falls in models considering ridge and valley and at last station which is 4.5 Km away from station 5. The frequency bandwidth for the generated Rayleigh wave is 0-12 Hz. But, the dominant frequency is around 4.0 Hz. There is minor ups and down in the horizontal component, this may be due to the presence of P-wave. It appears that the ratio of spectra of vertical to horizontal component is same for all the frequency near the epicentre. As it is seen that there is negligible change in amplitude of Rayleigh wave after travelling 4.5 Km. This negligible change is due to the dampening effect of rock.This supports that Rayleigh wave is generating from the point source of S-wave at some depth (100 m).

3.3 SEISMIC RESPONSE OFSINGLE RIDGE AND VALLEY

To see the response of single ridge and single valley having different geometry various models have been considered named as TMR Model as triangular ridge model, TMV Model as triangular valley model, EMR Model as elliptical ridge model, EMV Model as elliptical valley model and to analyze the Rayleigh wave characteristics, I have evaluated the effects on particle velocity, spectral amplification and spectral ratio with respect to HOMO Model at various points.

Points considered during analysis is station 5 which is at the crest of the ridge in TMR and EMR Model and at bottom of valley in TMV and EMV Model respectively and last station in TMR, TMV, EMR, EMV Models. We have considered ridge of height 360m and width 720m and valley of depth 360m and width 720m.

3.3.1 Seismic response of single triangular ridge

Figure 3.5 shows the single triangular ridge (TMR) model along with source and receiver array. The seismic response of the TMR model is shown in figure 3.6 for both the components. The analysis of this figure depicts the reflected and the transmitted Rayleigh waves as well as the diffracted P- and SV-waves from the ridge topography.Further, just after the ridge topography the recorded phases are incident P-wave, diffracted P-wave, diffracted SV-wave and the transmitted two phases of the Rayleigh waves. It appears that the triangular ridge has caused the splitting of the transmitted Rayleigh wave. The analysis of the trace just at the top of the ridge (shown by red color) depicts that the horizontal component gets amplified and vertical component gets de-amplified at the ridge crest compared to homogeneous topography.

The sudden increase of amplitude of horizontal component of Rayleigh wave near the top of the ridge calls for the polarization analysis since the horizontally polarized Rayleigh wave may trigger the landslides under favourable condition.

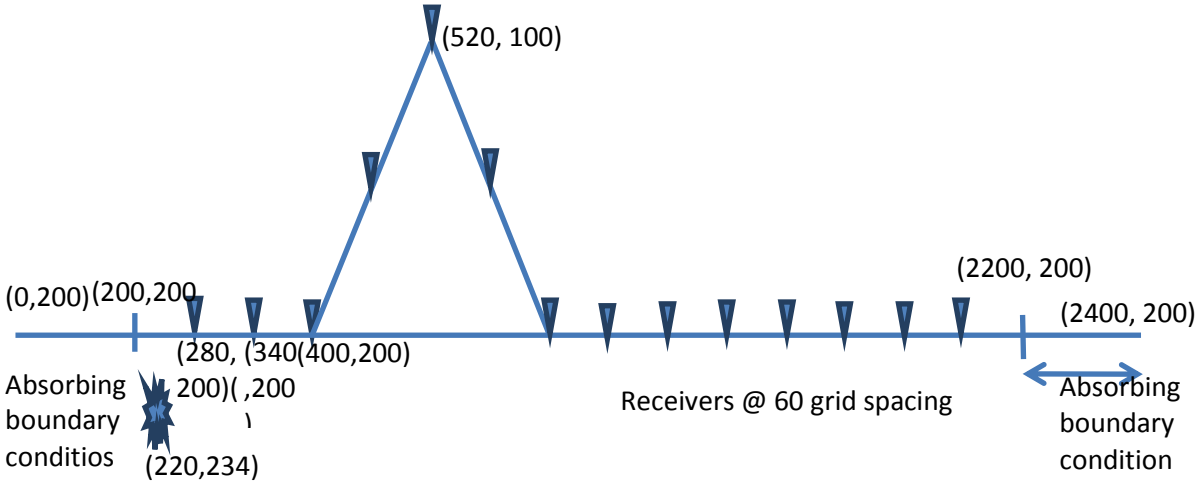

Figure 3.4 TMR Model

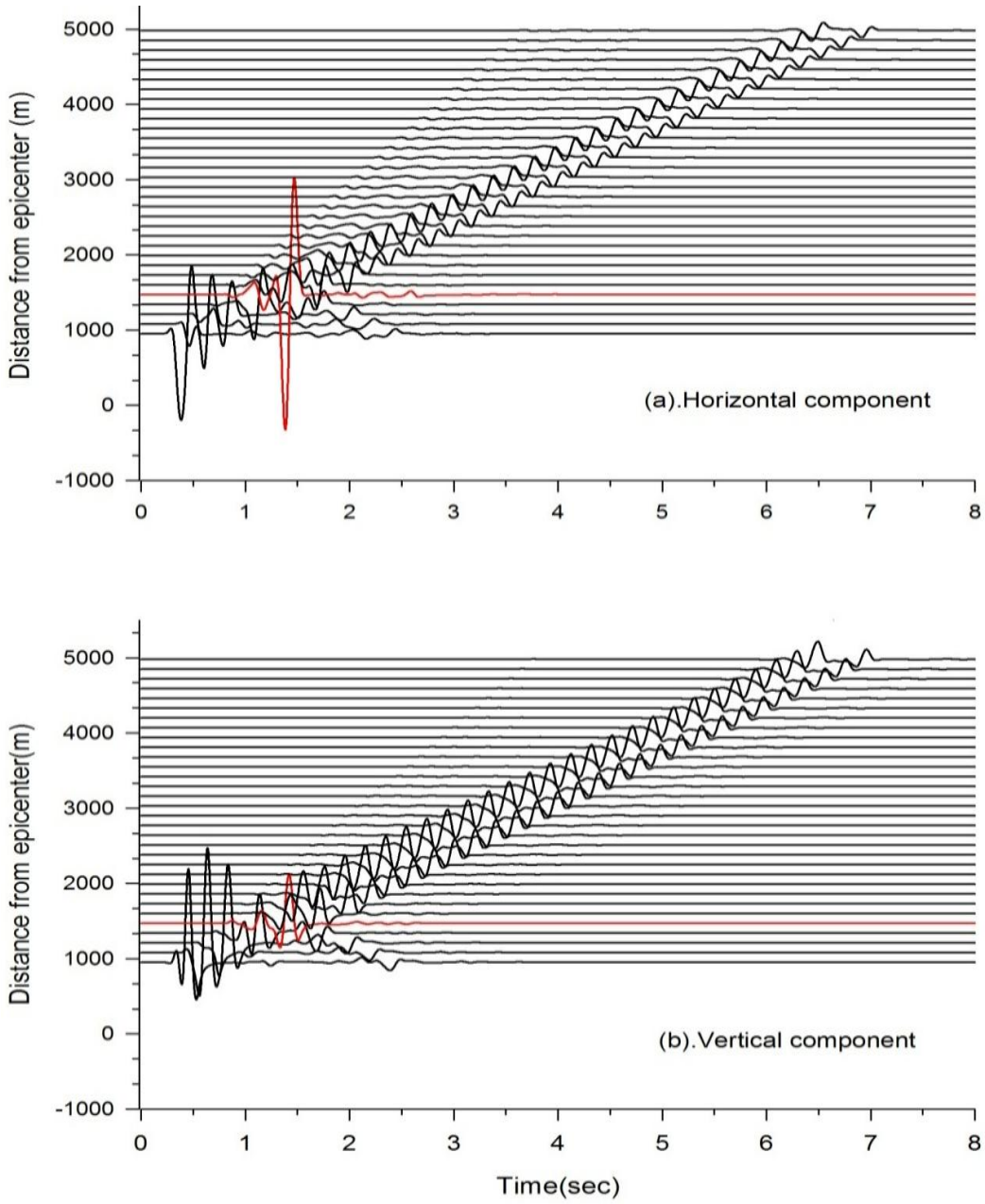

Fig.3.5Horizontal and vertical component of Particle velocity response of TMR Model

Figure 3.6 shows the spectra of horizontal and the vertical components of response of the TMR model at two locations. The spectral ratio of the corresponding traces with respect to the HOMO model is shown in figure 3.8. The analysis of this figure depicts very large amplification of the horizontal component and de-amplification of the vertical component at the ridge top. At the last station, the spectral ratio for both the components is same. This reflects overall decrease of the Rayleigh wave amplitude due to the insulating effects of the ridge topography on the Rayleigh waves. It appears that the insulating effect is larger for the larger frequency of the Rayleigh waves.

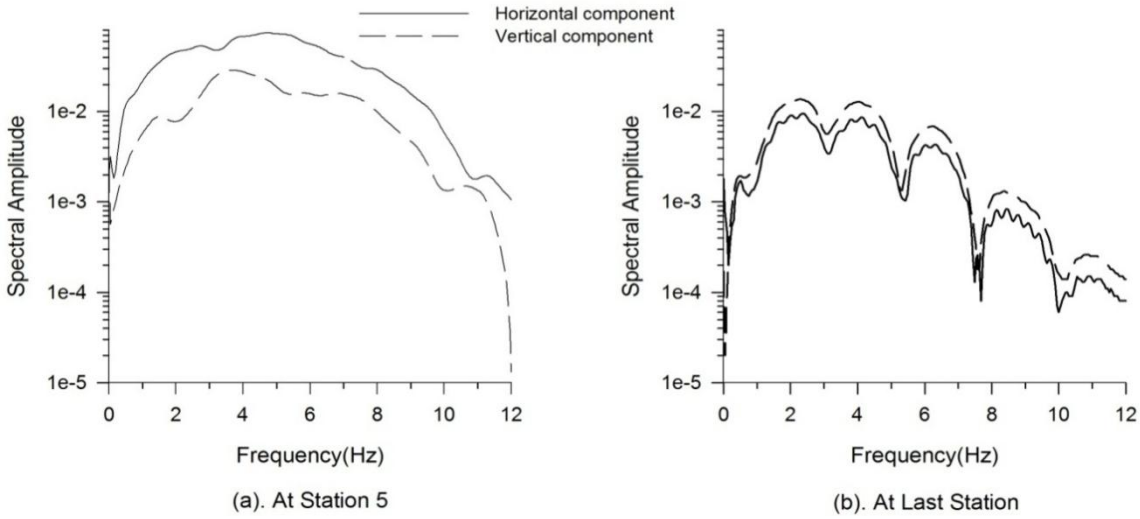

Fig.3.6Spectral amplitude of the horizontal and the vertical components at two location corresponding to the responses of the TMR Model.

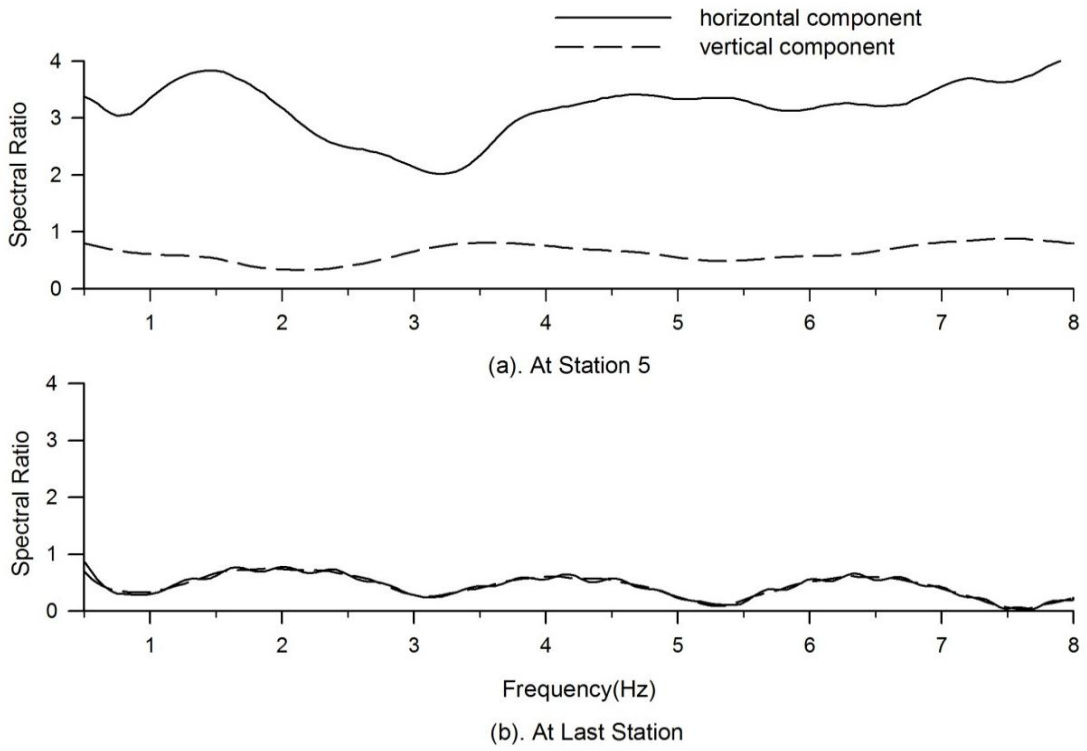

Fig. 3.7 Spectral Ratio of horizontal and vertical components of response of TMR model at two location with respect to HOMO Model

3.3.2 Snapshots at different moments

To infer the behavior of the Rayleigh after interacting with the ridge topography, snapshots have been computed in a rectangular area at different moments and shown in figure 3.8 for both horizontal (left) and the vertical (right) components.In the snapshots at time 2.7 sec,the Rayleigh wave has just entered into the model having high amplitude in vertical direction and showing the nature of Rayleigh wave in homogeneous medium. In the snapshot at time 3.9 sec, the Rayleigh wave reached the crest of the ridge. As it is clearly visible that horizontal component gets strongly amplified and vertical component gets de-amplified. It means that at the crest of the ridge the Rayleigh wave becomes horizontally polarized.

As the wave passes the topography, the Rayleigh wave splits into two component as can be easily seen in the snap at time 4.5 sec and reflected Rayleigh wave are also generated. A significant proportion of diffracted P- wave and diffracted S- wave also generated which moves downward in the form of circular wavefront showing the nature of body wave.

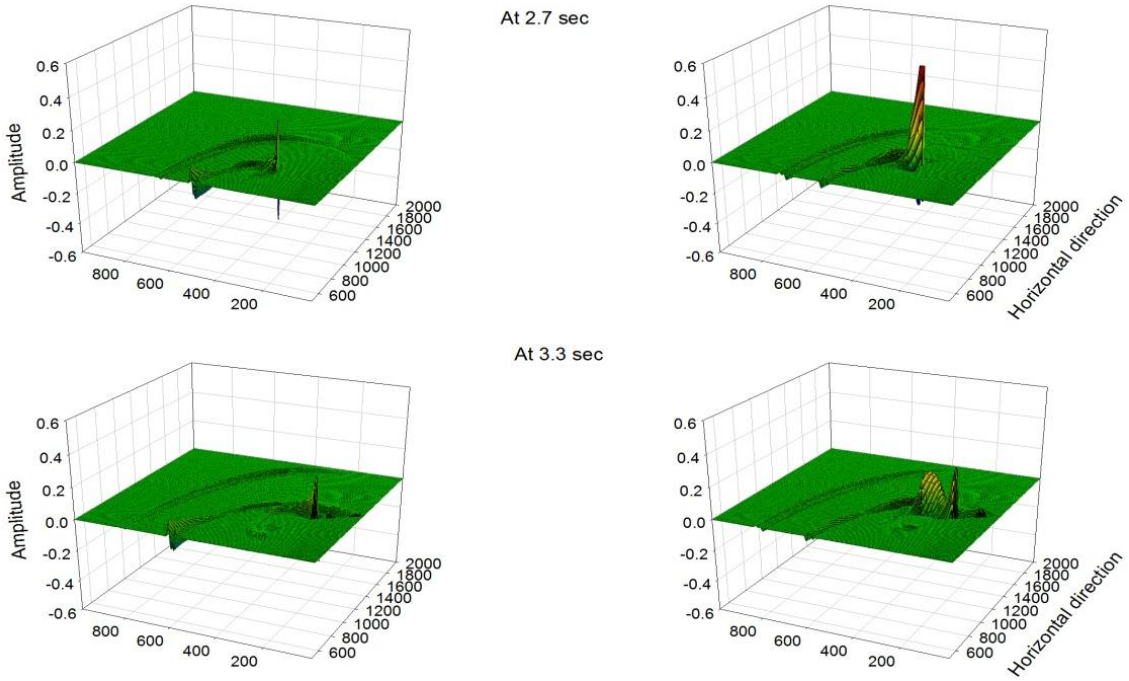

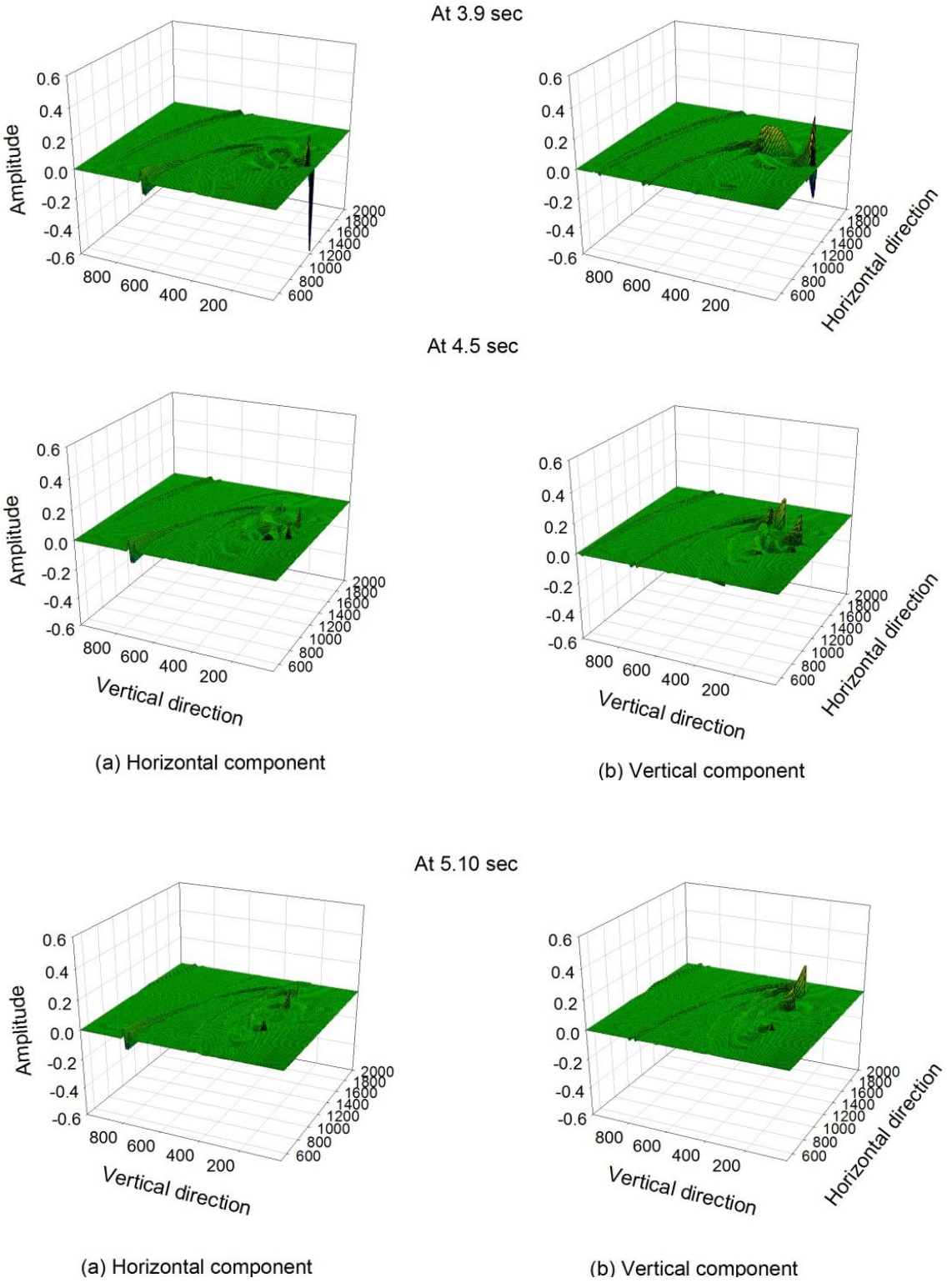

Fig 3.8 Snapshot of Rayleigh wave at different moments for TMR model.

3.3.3 Seismic response of single triangular valley

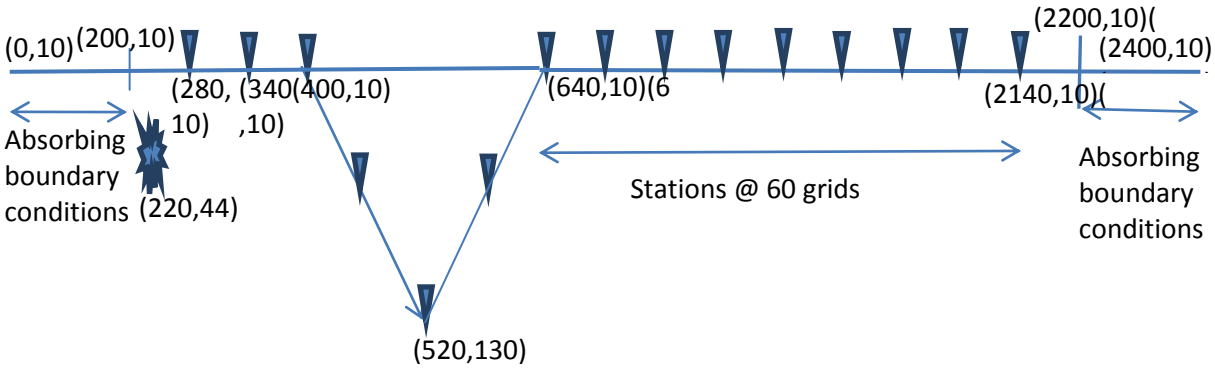

Figure 3.9TMV Model

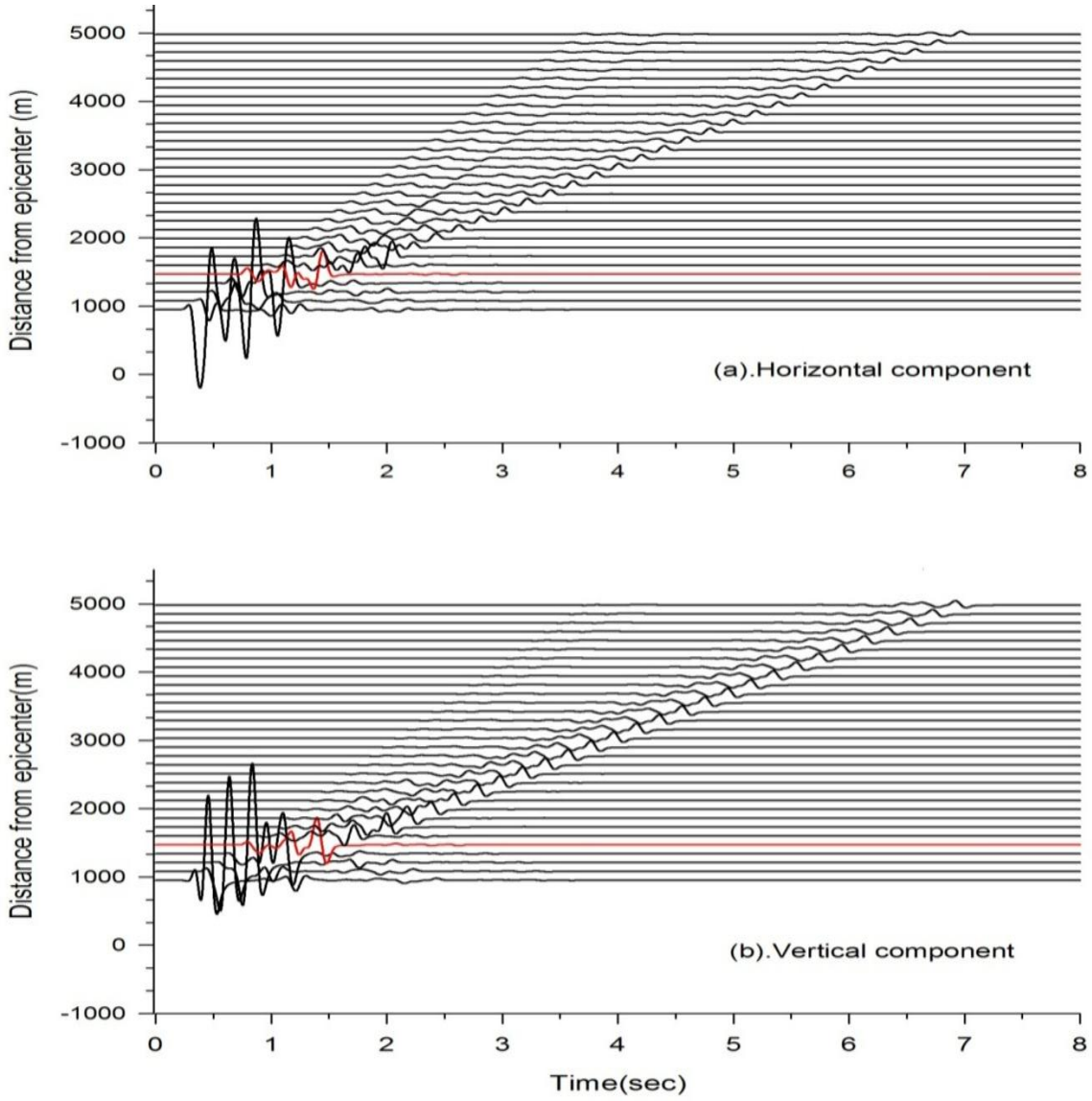

Fig.3.10Horizontal and vertical component of Particle velocity response of TMV Model

Figure 3.9 shows the single triangular valley (TMV) model along with source and receiver array. The seismic response of the TMV model is shown in figure 3.11 for both the components. The analysis of this figure depicts the reflected and the transmitted Rayleigh waves as well as the diffracted P- and SV-waves from the valley.Further, just after the ridge topography the recorded phases are incident P-wave, diffracted P-wave, diffracted SV-wave and the transmitted two phases of the Rayleigh waves. It appears that the triangular valley has also caused the splitting of the transmitted Rayleigh wave. The analysis of the trace just at the base of valley (shown by red color) depicts that the both the components get de-amplified.

Figure 3.11 shows the spectra of horizontal and the vertical components of response of the TMV model at two locations. The spectral ratio of the corresponding traces with respect to the HOMO model is shown in figure 3.12. The analysis of this figure depicts the deaplification of both the component at the base of valley. At the last station, the spectral ratio for both the components is same as was seen in case of ridge. This also reflects overall decrease of the Rayleigh wave amplitude due to the insulating effects of the valley on the Rayleigh waves. It appears that the insulating effect caused by the valley is larger than that caused by the ridge. Hence we can recommend to build up the houses near to the valley areas as it is acting as an insulator to Rayleigh wave rather near to the ridge.

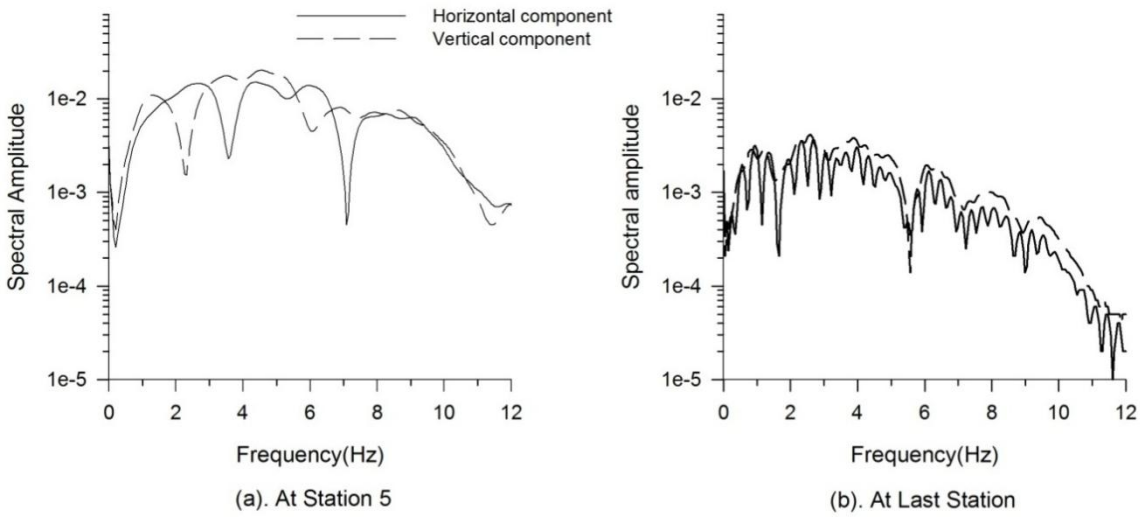

Fig.3.11Spectral amplitude of the horizontal and the vertical components at two location corresponding to the responses of the TMV Model

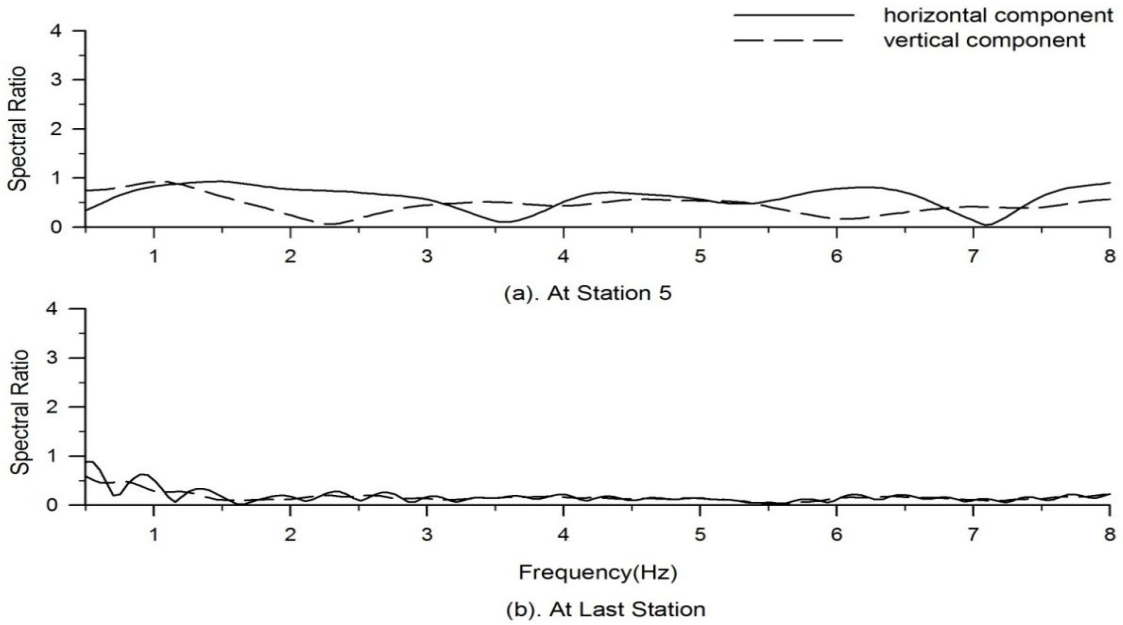

Fig. 3.12Spectral Ratio of horizontal and vertical components of response of TMV model at two location with respect to HOMO Model

3.3.4 Seismic response of single elliptical ridge

Figures 3.13-3.15 show the EMR, its response and the spectral ratios at two locations wrt to the HOMO model. Similarly, figures 3.17-3.19 show the EMV model, its response and the spectral ratios at two locations wrt to the HOMO model. The analysis of these figures reflects that the insulating effects of elliptical ridge and valley models is lesser to that of triangular models.

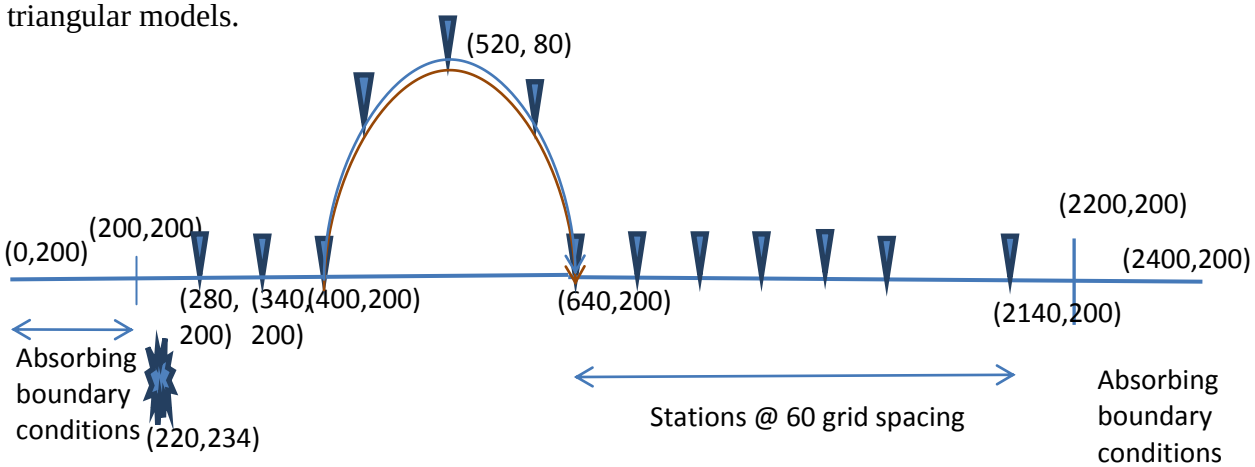

Figure 3.13 EMR Model

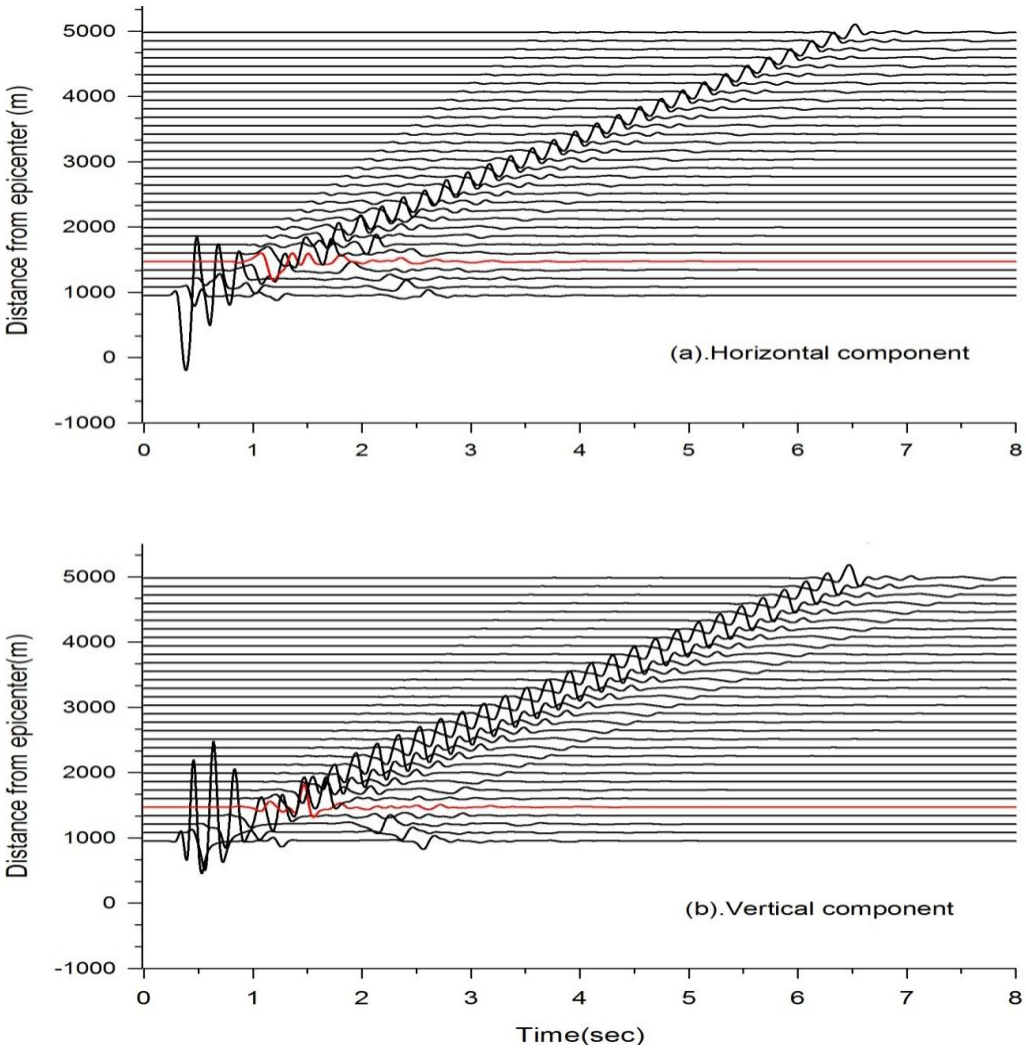

Fig.3.14Horizontal and vertical component of Particle velocity response of EMR Model

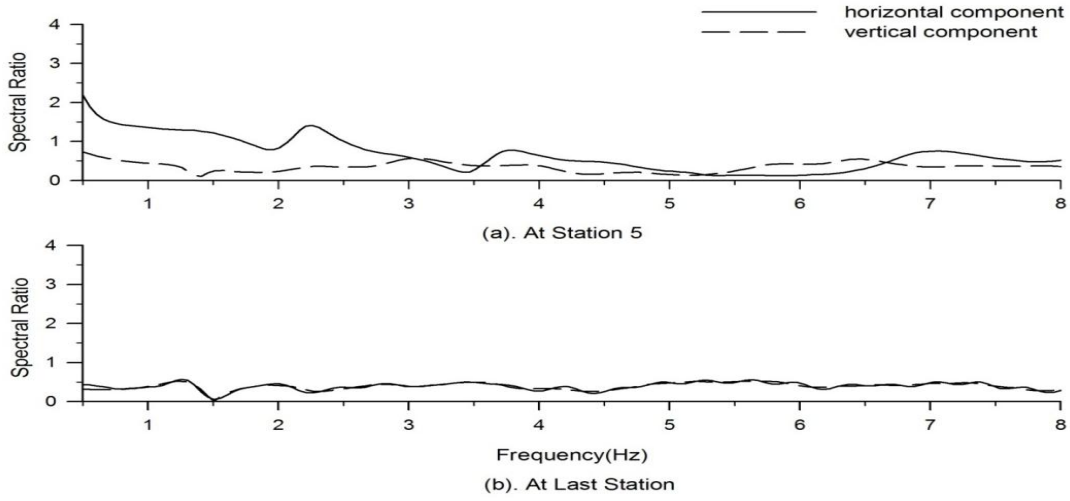

Fig. 3.15Spectral Ratio of horizontal and vertical components of response of EMR model at two location with respect to HOMO Model

In case of elliptical ridge there is no significant increase in amplitude of horizontal component but the vertical component decreases at the faster rate as in case of triangular ridge model. At the last station energy remain in the Rayleigh wave is very comparable to the case of triangular valley but slightly more than that.

3.3.5 Seismic response of single elliptical valley

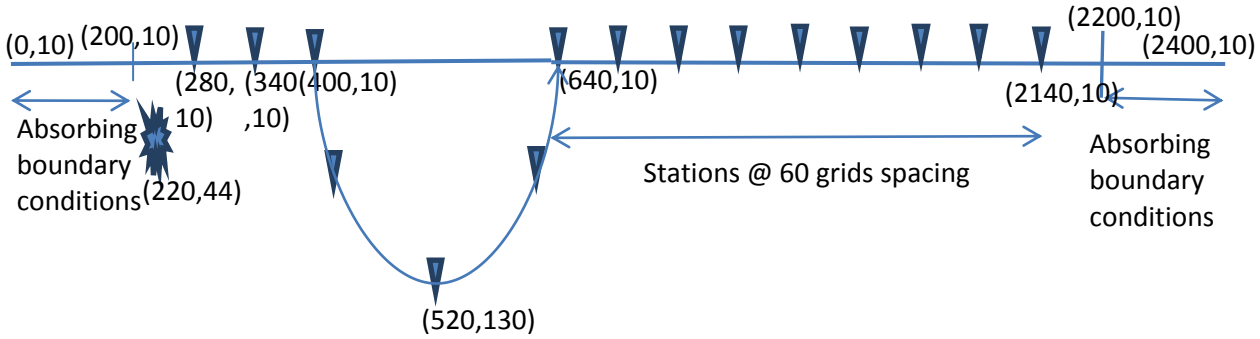

Figure 3.16 EMV Model

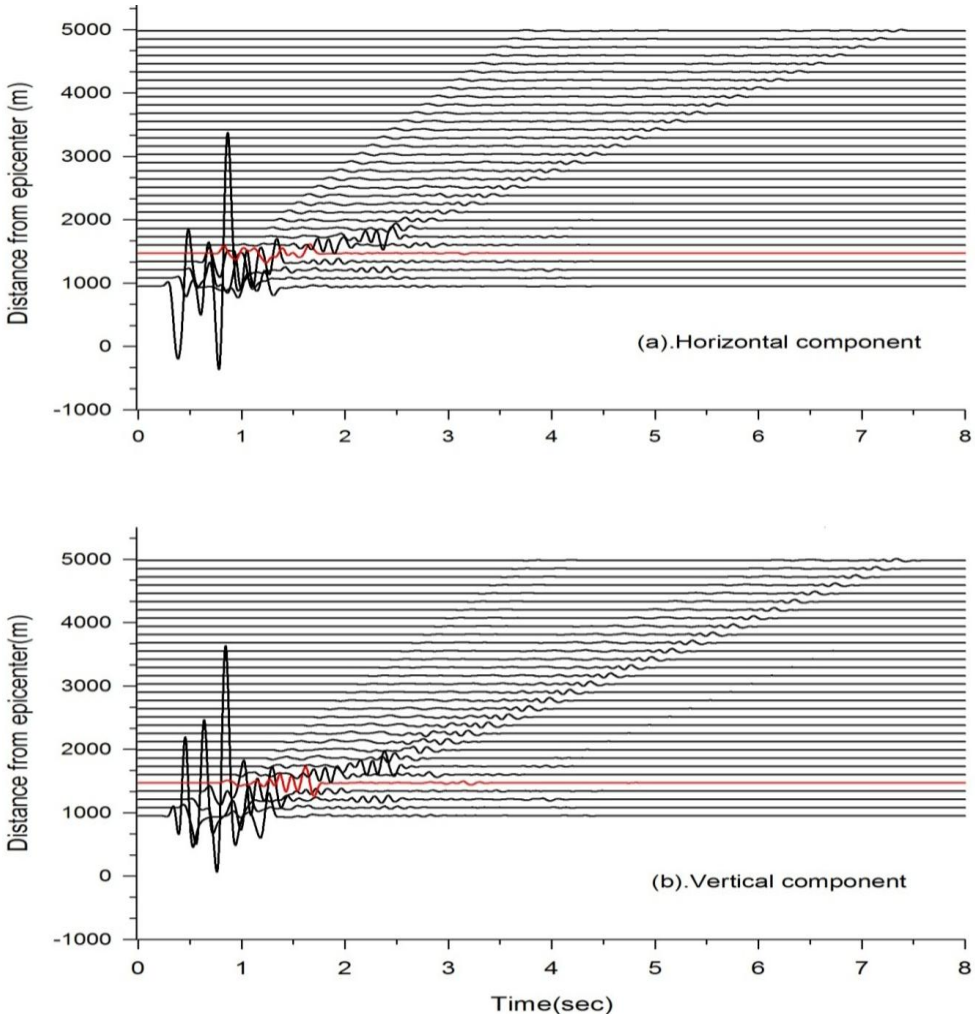

Fig.3.17 Horizontal and vertical component of Particle velocity response of EMV Model

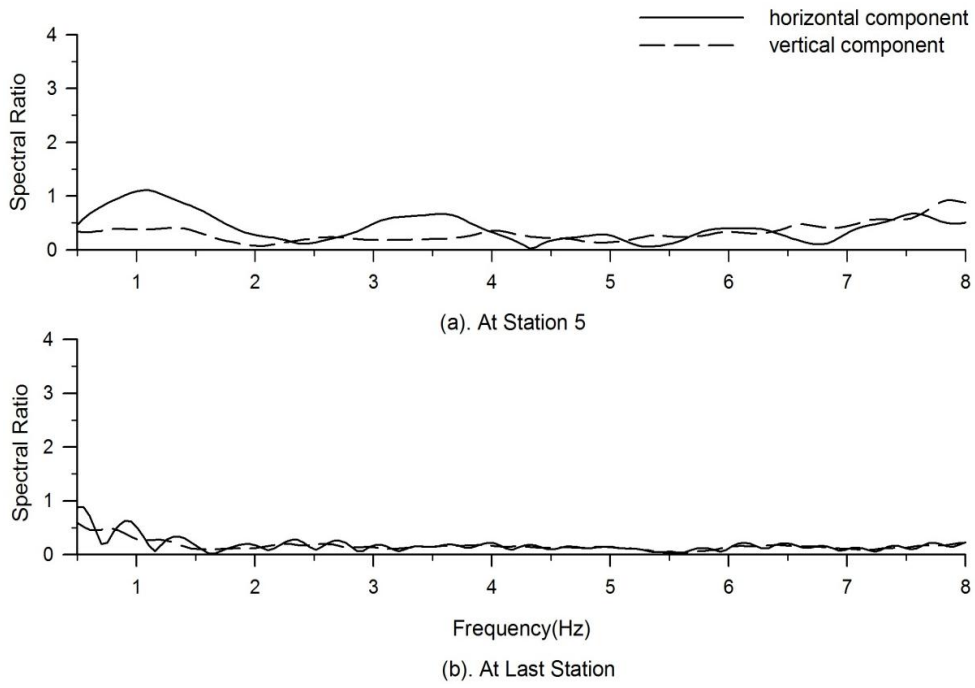

Fig. 3.18Spectral Ratio of horizontal and vertical components of response of EMV model at two location with respect to HOMO Model

3.4 ANALYSIS OF RESPONSES BEFORE AND AFTER CROSSING THE TOPOGRAPHY

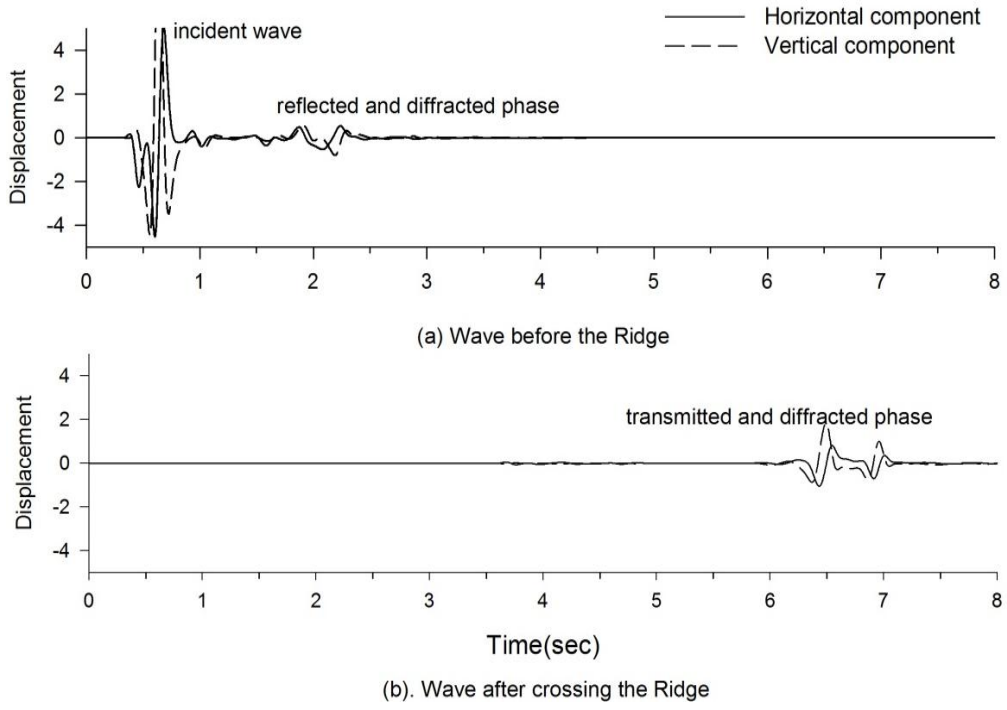

Fig. 3.19Showing different phases of wave before and after crossing the Ridge

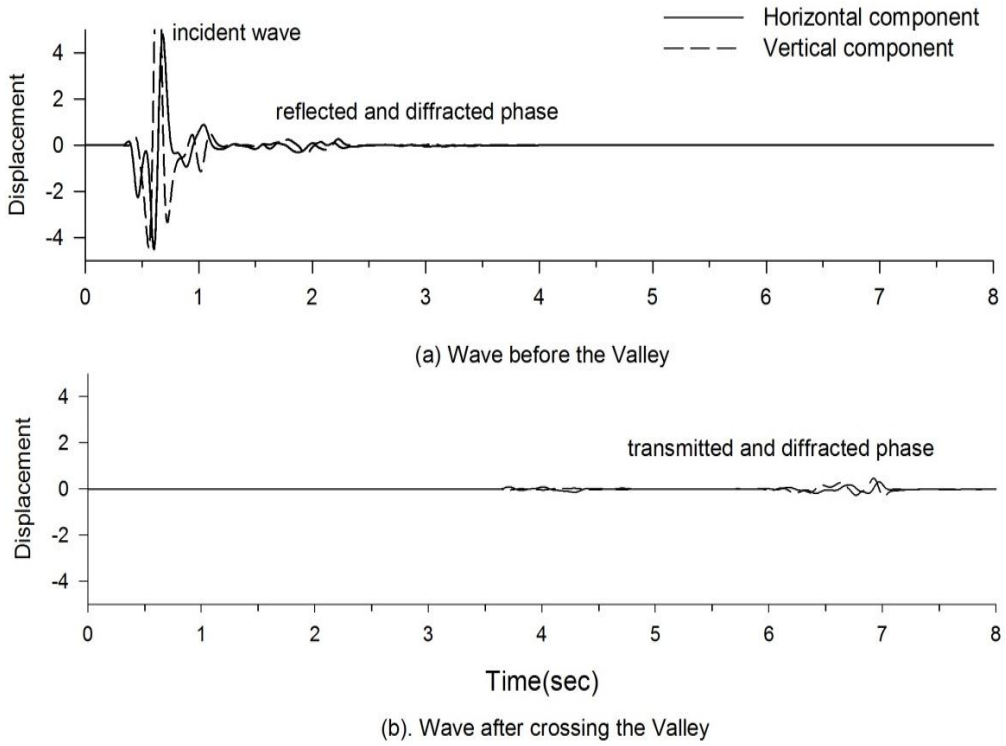

Fig. 3.20 Showing different phases of wave before and after crossing the Valley

Figure 3.19shows the components of Rayleigh wave before the topography and after crossing the topography in case of ridge and Figure 3.20 shows in case of valley. As it is seen from the figures that amplitude of reflected and transmitted phases after crossing the ridge is more than that after crossing the valley. Hence it can be concluded that valley absorbs the energy and de-amplify the amplitude of Rayleigh wave so it can be treated as sinking area whereas ridge amplify the amplitude of Rayleigh wave. We can also see two waves in transmitted signal and less amplitude diffracted waves in case of ridge but in case of valley two waves are not clearly visible hence diffraction is more.

3.5 EFFECTS OF SHAPE RATIO

Shape ratio is the ratio of height to half width. Change of geometry of the topography is also considered. Various models named ‘TLR and TLV Model’ as triangular low ridge and valley model of 240m height and 240m depth, 720m width respectively with shape ratio 0.67, ‘TMR and TMV Model’ as triangular medium ridge and valley model of 360m

height and 360m depth, 720m width respectively with shape ratio 1, 'THR and THV' Model as triangular high ridge and valley model of 585m height and 585m depth, 720m width respectively with shape ratio 1.625. Similarly models named 'ELR and ELV Model' as elliptical low ridge and valley model of 240m height and 240m depth, 720m width respectively with shape ratio 0.67, 'EMR and EMV Model' as elliptical medium ridge and valley model of 300m height and 300m depth, 720m width respectively with shape ratio 0.83, 'EHR and EHV Model' as elliptical high ridge and valley model of 360m height and 360m depth, 720m width respectively with shape ratio 1. Seismic responses of all the models have computed and analysis is done in terms of spectral amplitude, spectral ratio, averagespectral amplification.

3.5.1 SR-effect triangular ridge

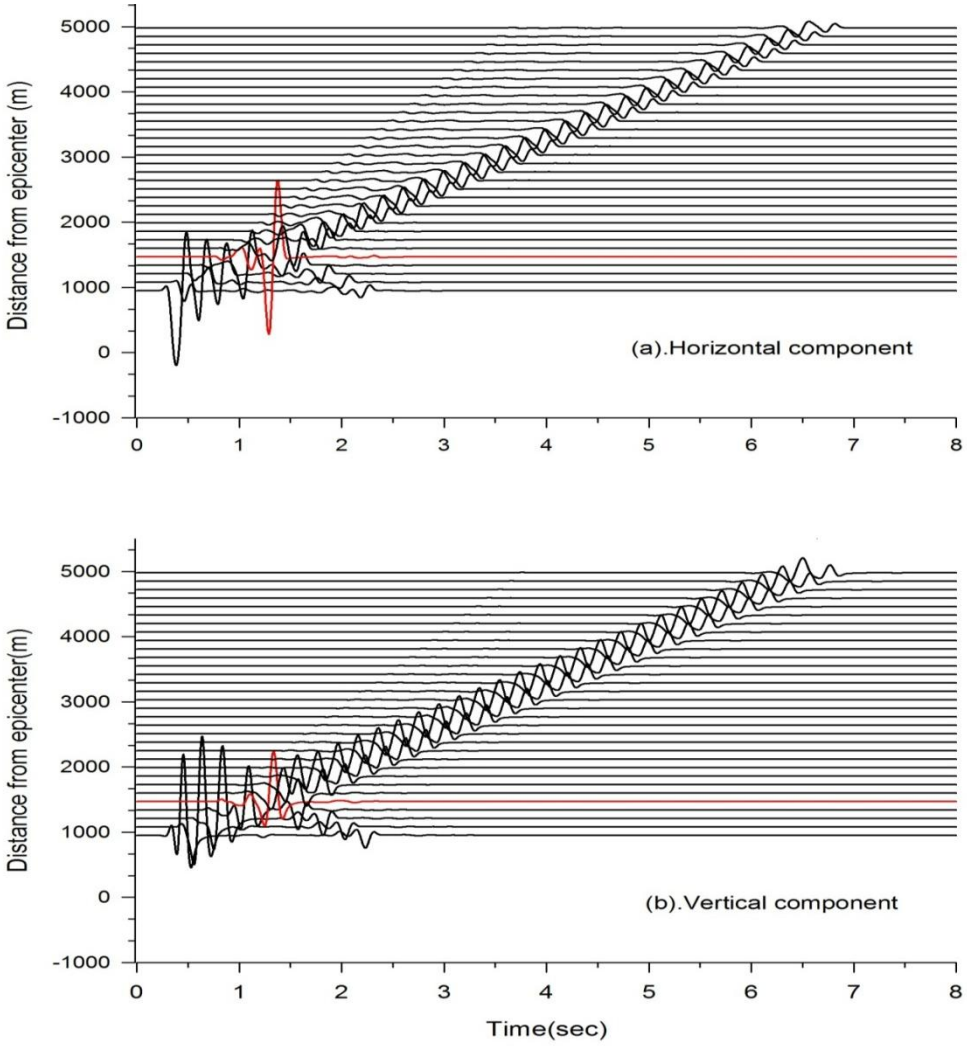

Fig.3.21Horizontal and vertical component of Particle velocity response of TLR Model

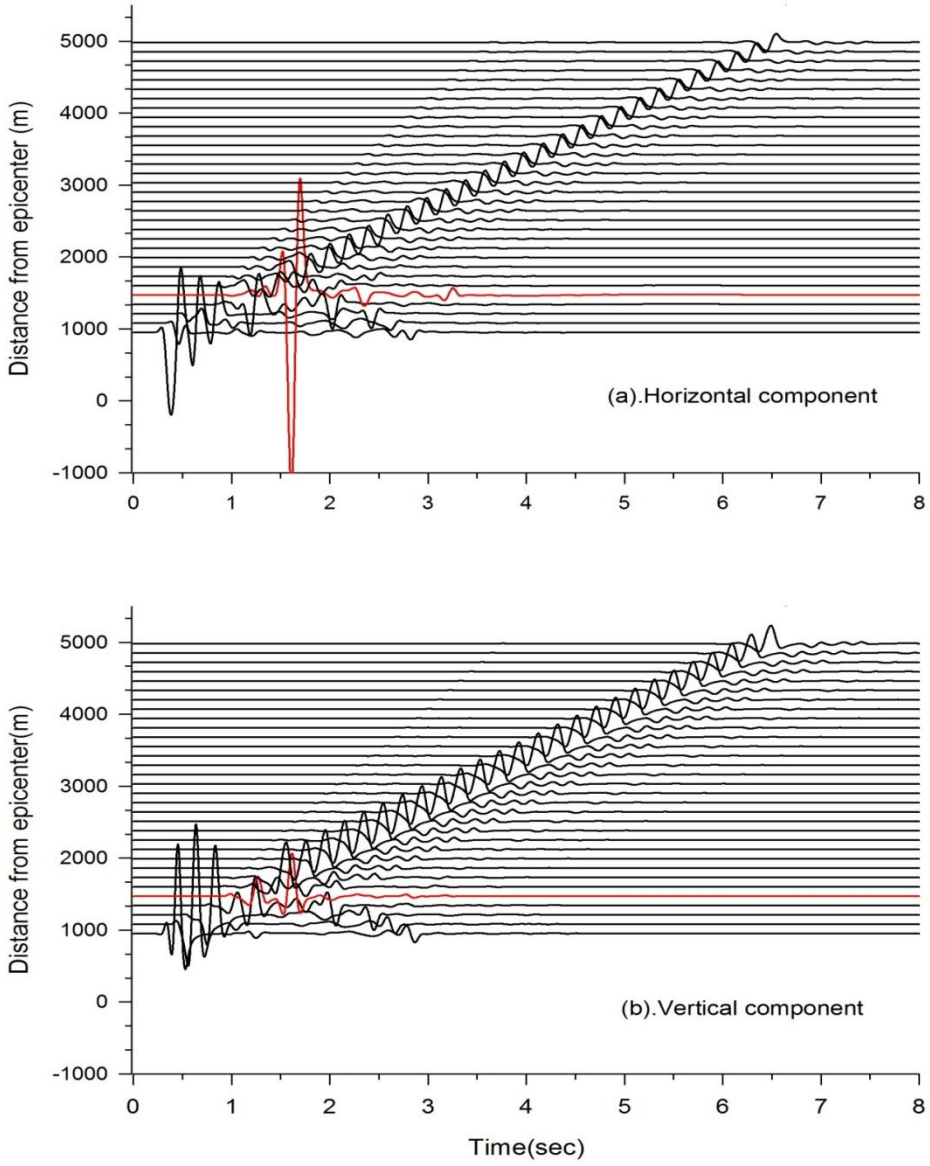

Fig.3.22Horizontal and vertical component of Particle velocity response of TMR Model

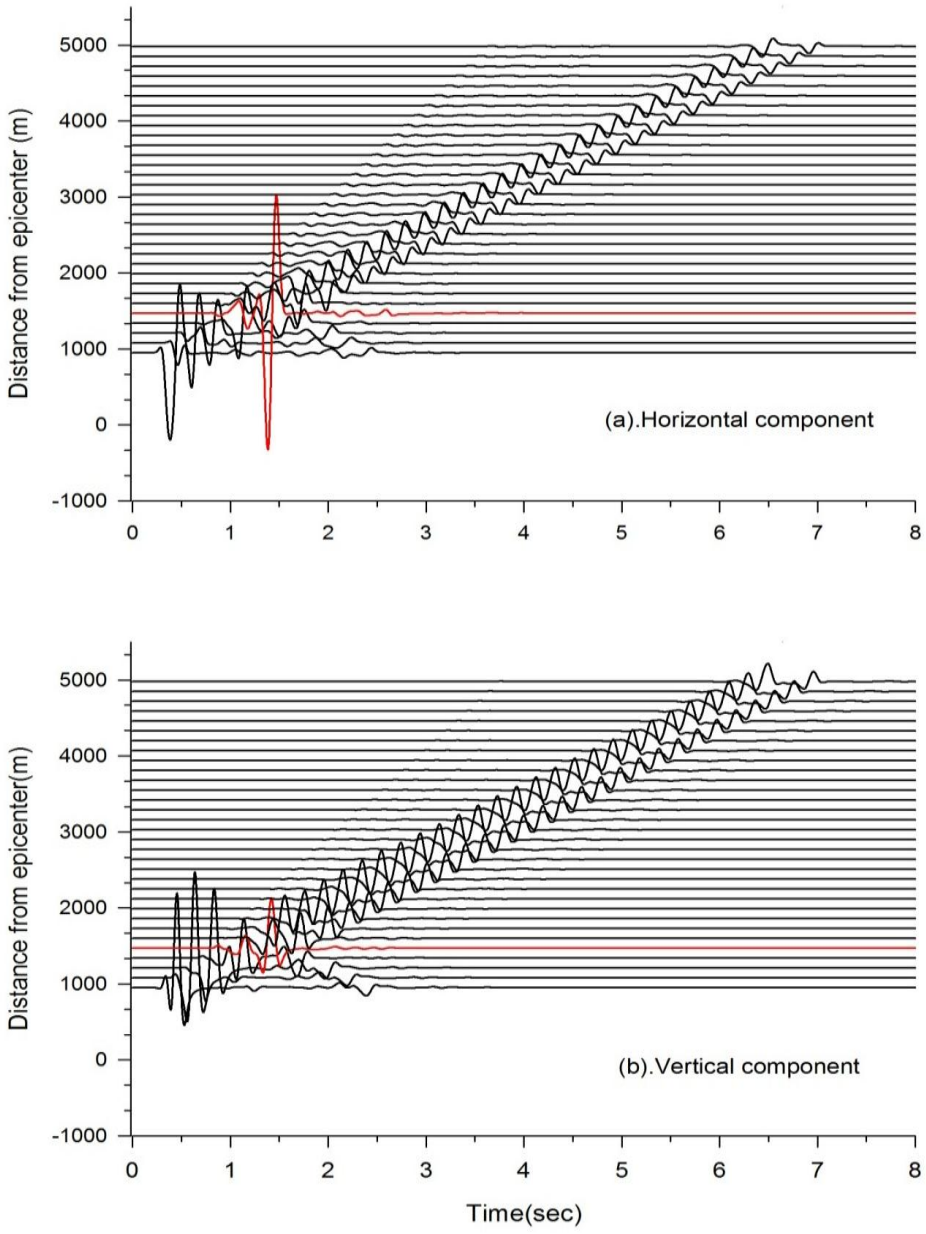

Fig.3.23Horizontal and vertical component of Particle velocity response of THR Model

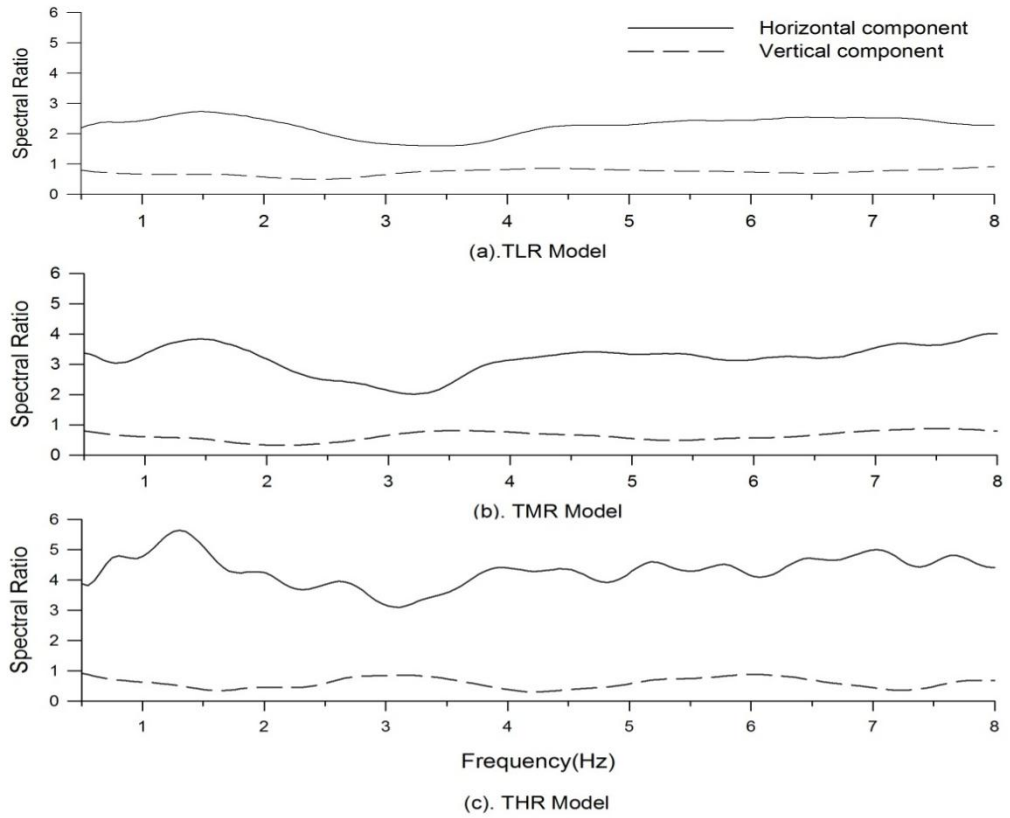

Fig. 3.24 Spectral ratio of various triangular ridge models at the crest of ridge compared with homogeneous model

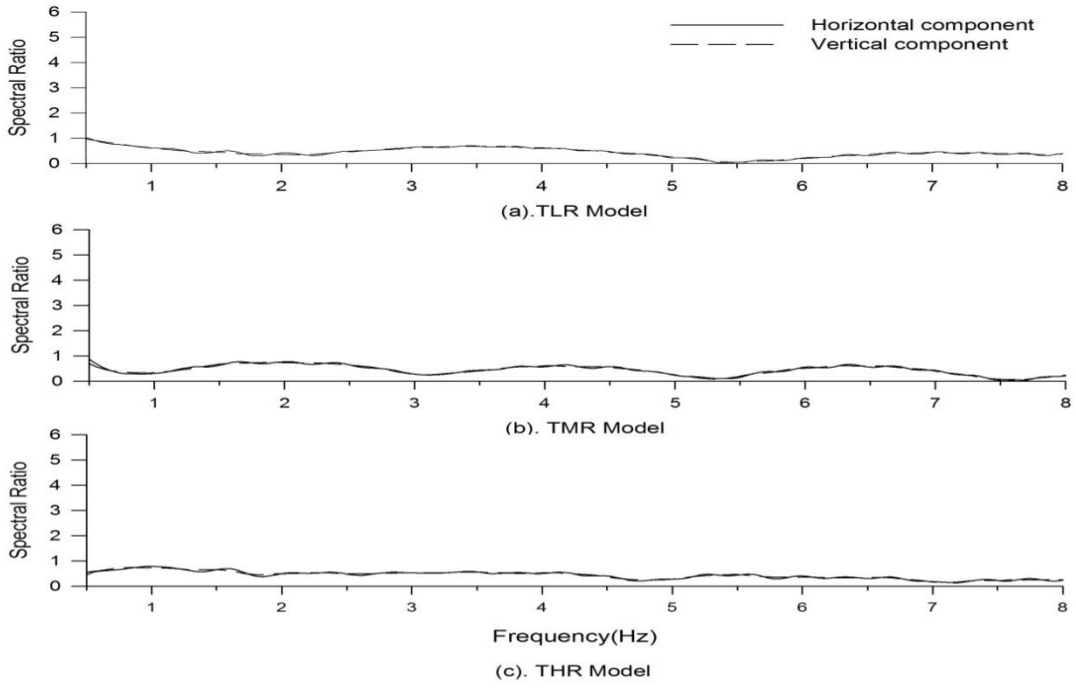

Fig. 3.25 Spectral ratio of various triangular ridge models at the last station compared with homogeneous model

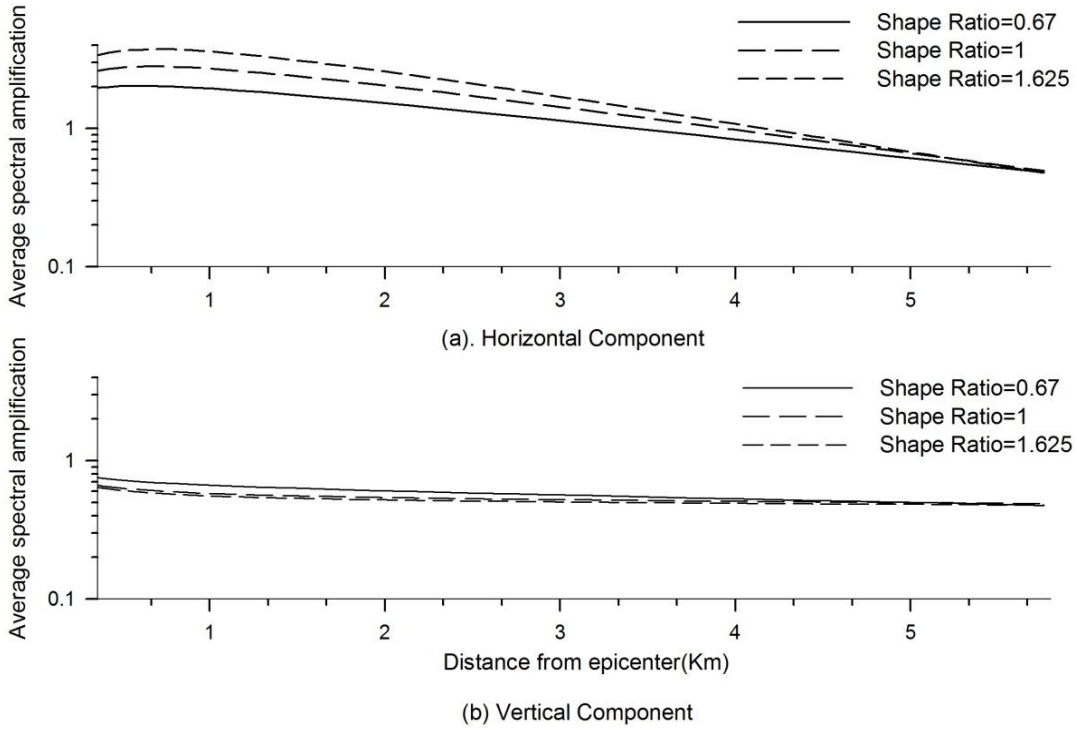

Fig. 3.26ASA of triangular ridge model comparing various shape ratio

Fig 3.21, 3.22, 3.23 shows the particle velocity at various shape ratio shows that amplification of horizontal component of Rayleigh wave increases and de-amplification of vertical component of Rayleigh wave increases with increase in shape ratio. Diffracted P-wave, diffracted S-wave and reflected R-wave also increases with increase in shape ratio.

At the last station energy in the Rayleigh wave not decreases to a significant amount.it contains energy even at the last station. Amplification of horizontal component is very large it may leads to the hazards like landslides, etc.

3.5.2 SR-effect triangular valley

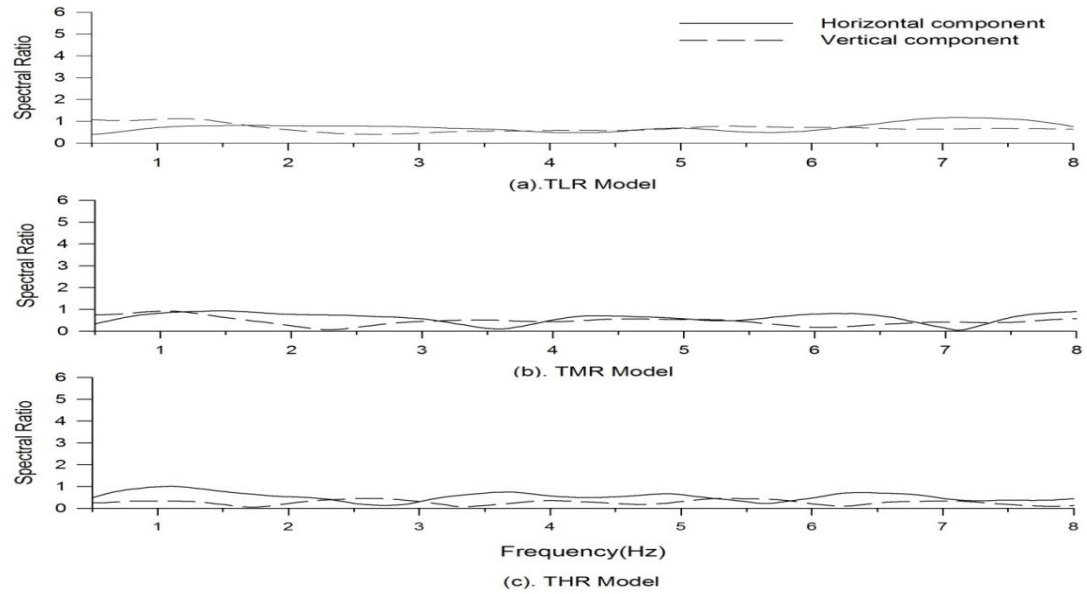

Fig. 3.27 Spectral ratio of various triangular valley models at the bottom of valley compared with homogeneous model

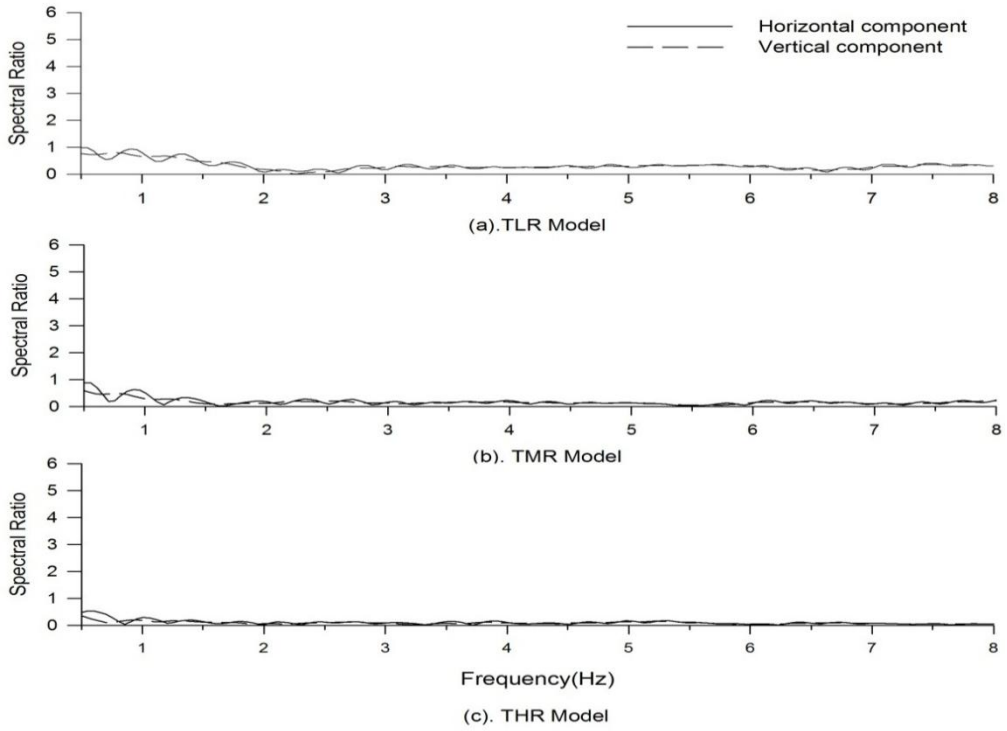

Fig. 3.28 Spectral ratio of various triangular valley models at the last station compared with homogeneous model

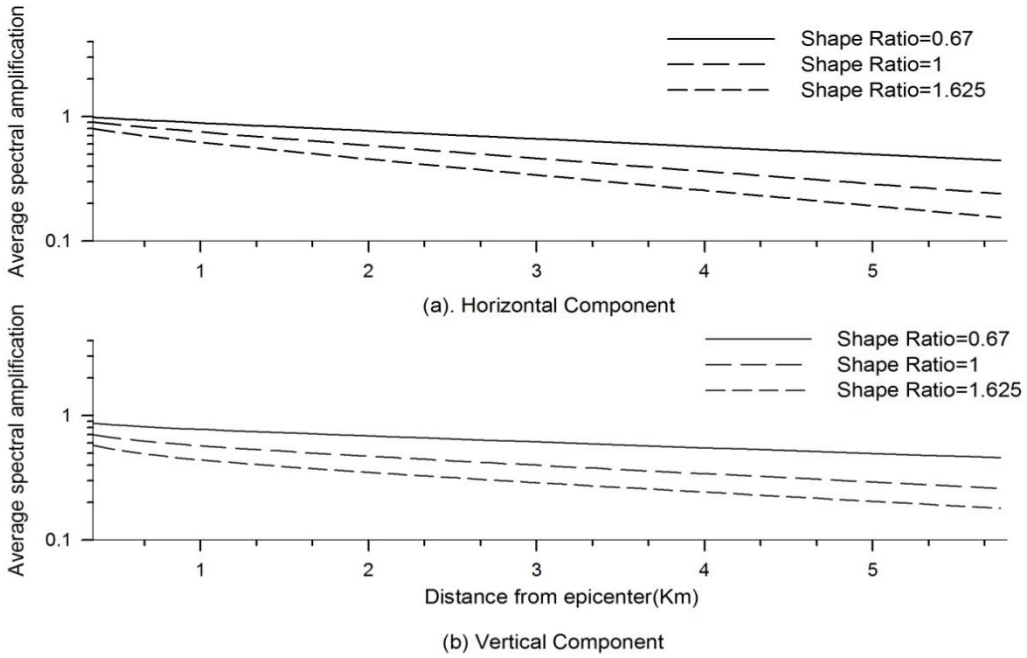

Fig. 3.29 ASA of triangular valley model comparing various shape ratio

Analysis from the figures depicts that both the horizontal and vertical component of Rayleigh wave gets de-amplified at the bottom of the valley but the rate of de-amplification of the horizontal component is more than that of vertical component. This rate of de-amplification increases with increase in shape ratio. Diffracted P-wave, diffracted S-wave and reflected R-wave also increases with increase in shape ratio.

As the depth of the valley increases the energy in the signal at last station goes on decreasing. There is negligible energy in the higher frequency signal i.e the valley is absorbing the high frequency signal and acting as a sinking zone.

3.5.3 SR- effect elliptical ridge

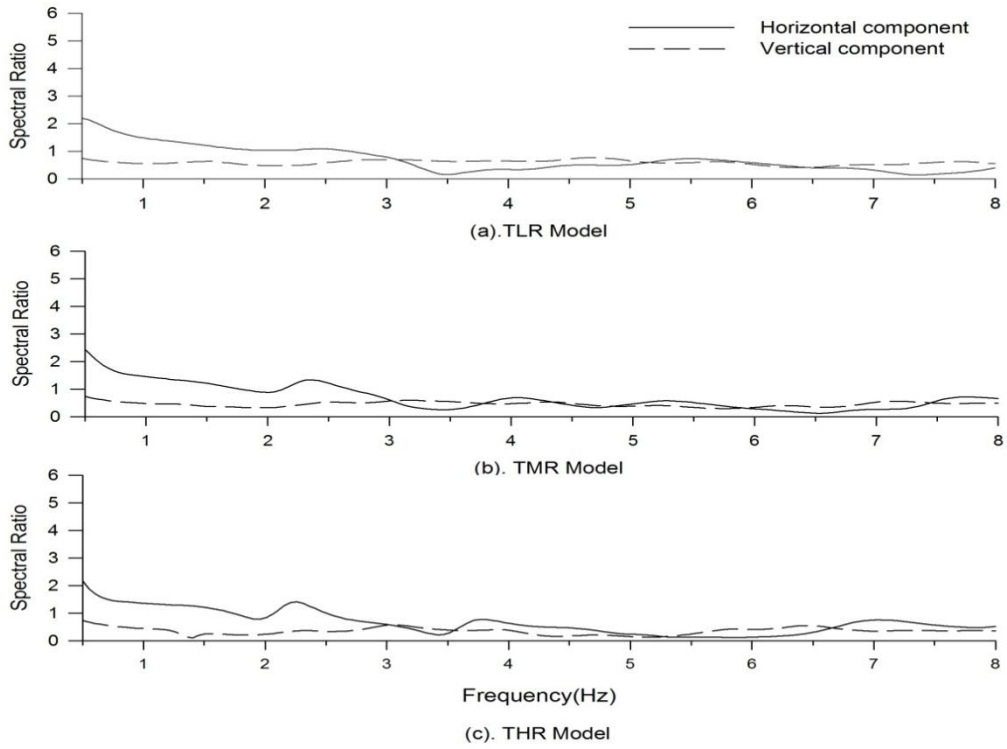

Fig. 3.30 Spectral Ratio of various elliptical ridge models at the crest of ridge when compared with homogeneous model

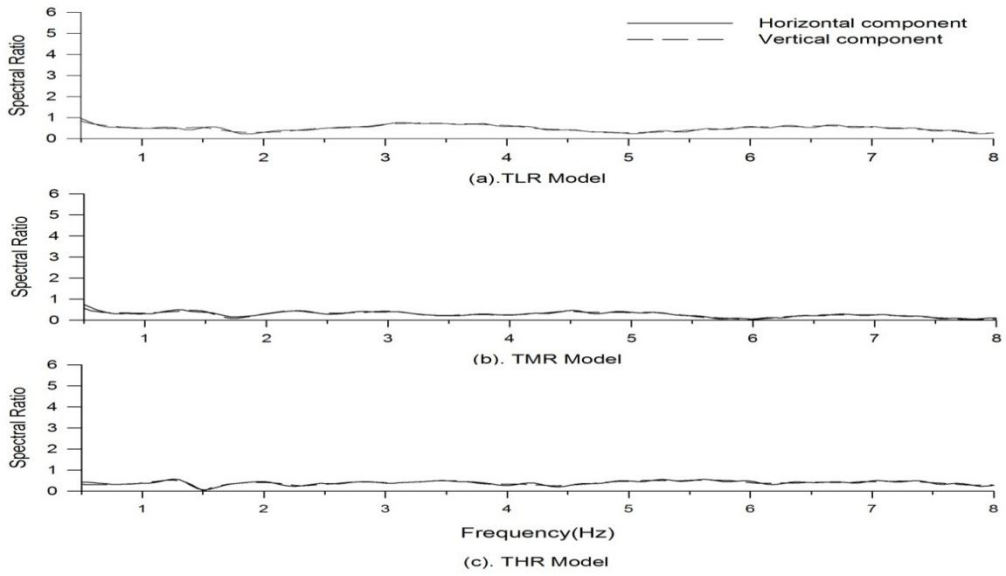

Fig. 3.31 Spectral Ratio of various elliptical ridge models at the last station when compared with homogeneous model

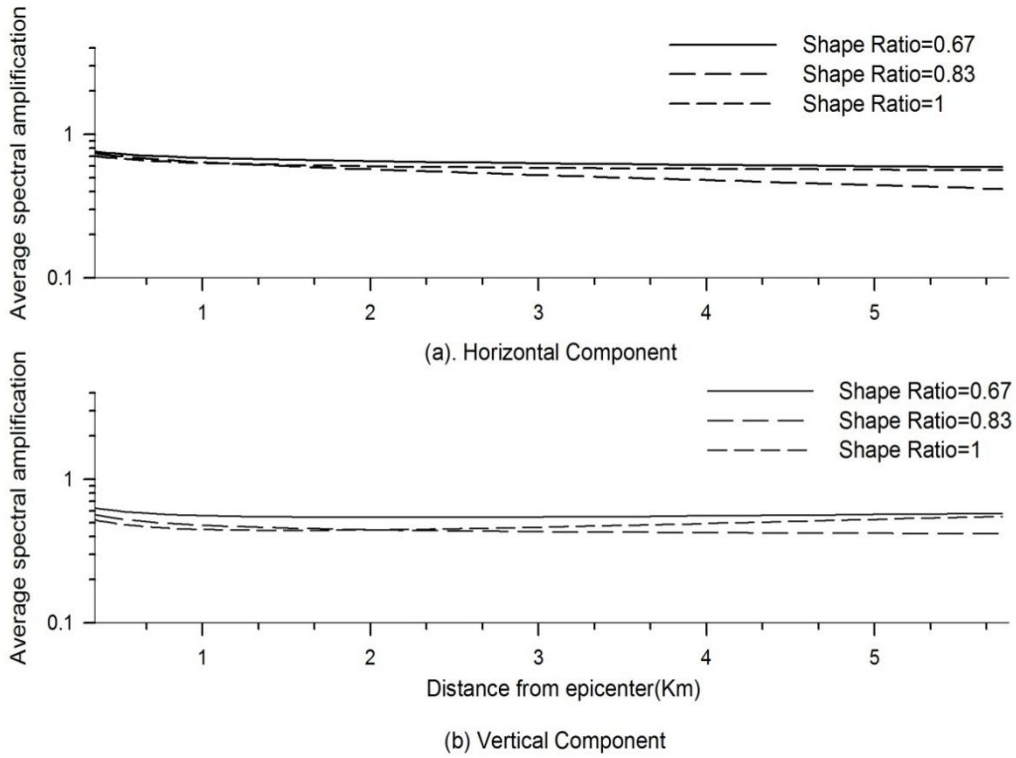

Fig. 3.32 ASA of elliptical ridge model comparing various shape ratio

Fig 3.31 shows spectral ratio at the last station. Energy in the wave is very less hence elliptical shape of topography also helps in dampening the effect of Rayleigh wave. From the above figures it is inferred that amplitude of both horizontal and vertical component decreases with increase in shape ratio. But the effect of increasing height in case of elliptical ridge is not significantly changing the nature of Rayleigh wave. Response is nearly same at different shape ratio.

3.5.4 SR- effect elliptical valley

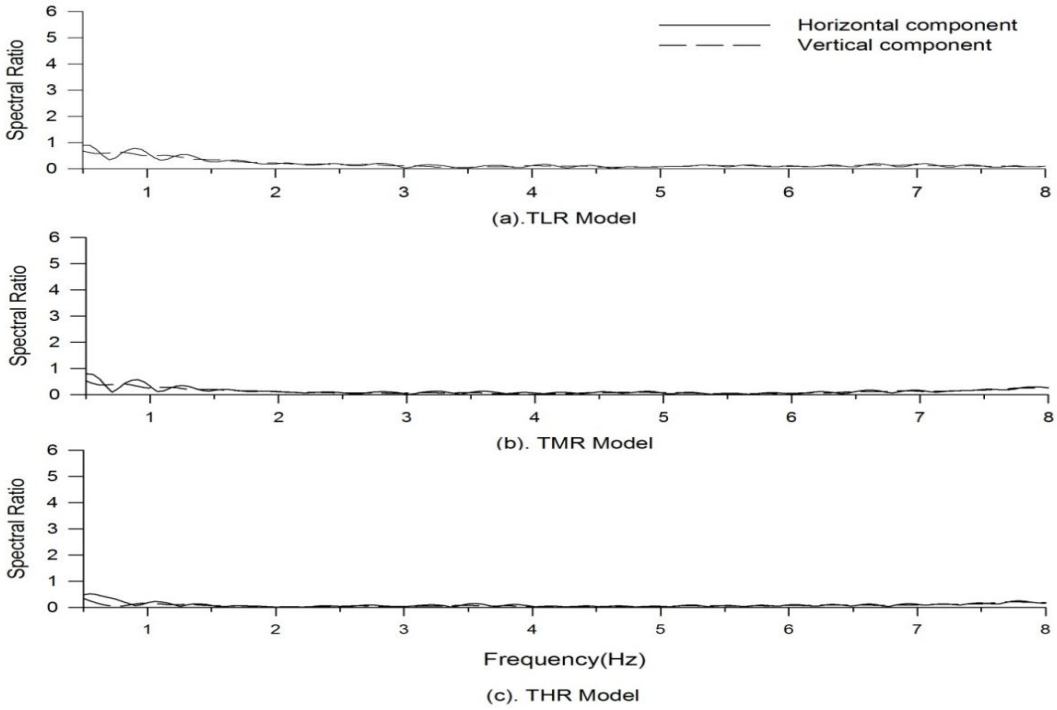

Fig. 3.33 Spectral Ratio of various elliptical valley models at bottom of valley when compared with homogeneous model

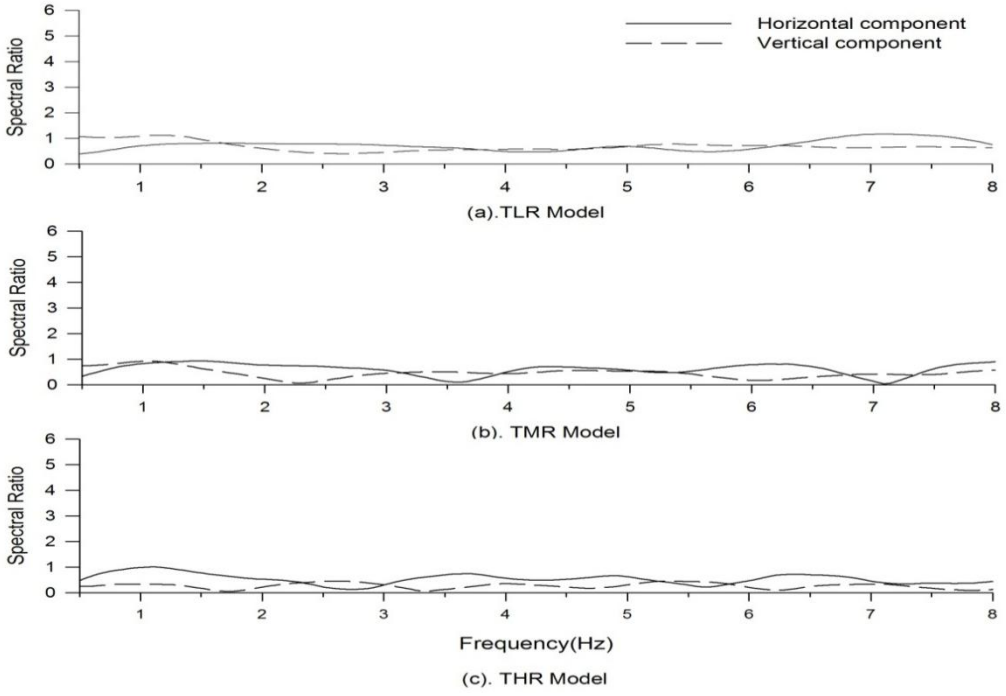

Fig. 3.34 Spectral Ratio of various elliptical valley models at the last station when compared with homogeneous model

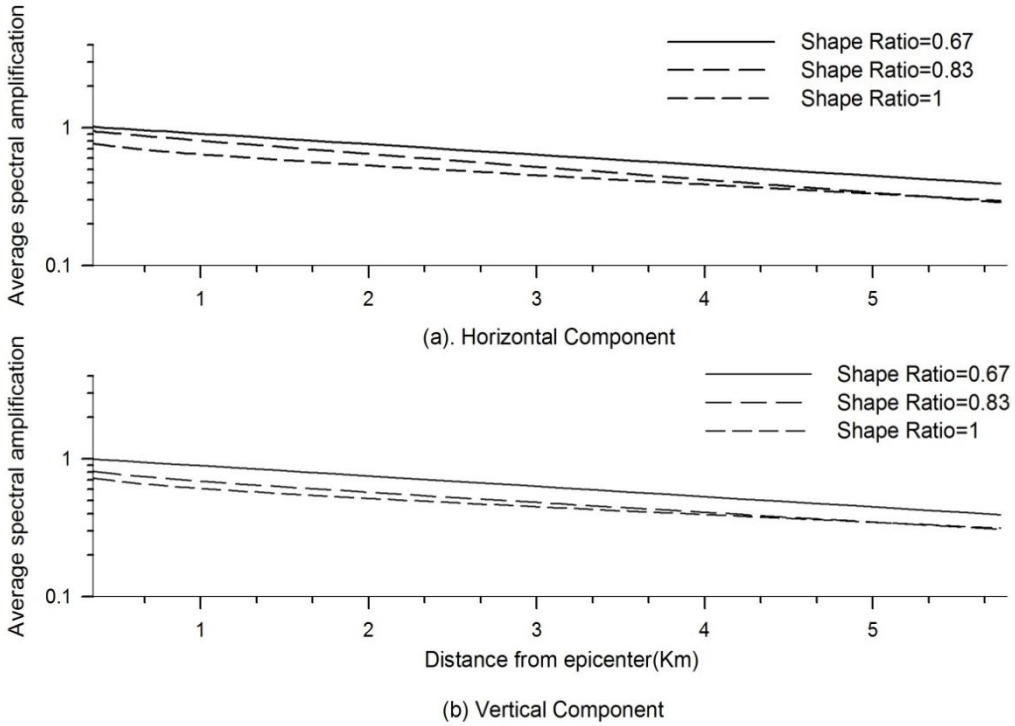

Fig. 3.35 ASA of elliptical valley model comparing various shape ratio

In case of ellipticalamplitude ofboth the horizontal and vertical component decreasebut the rate of decrease is more than that of elliptical ridge but less than that in case of triangular valley model. This rate of decrease, increases with increase in shape ratio.

3.5.5 TIME SEPARATION AFTER THE INTERACTION WITH THE TOPOGRAPHY

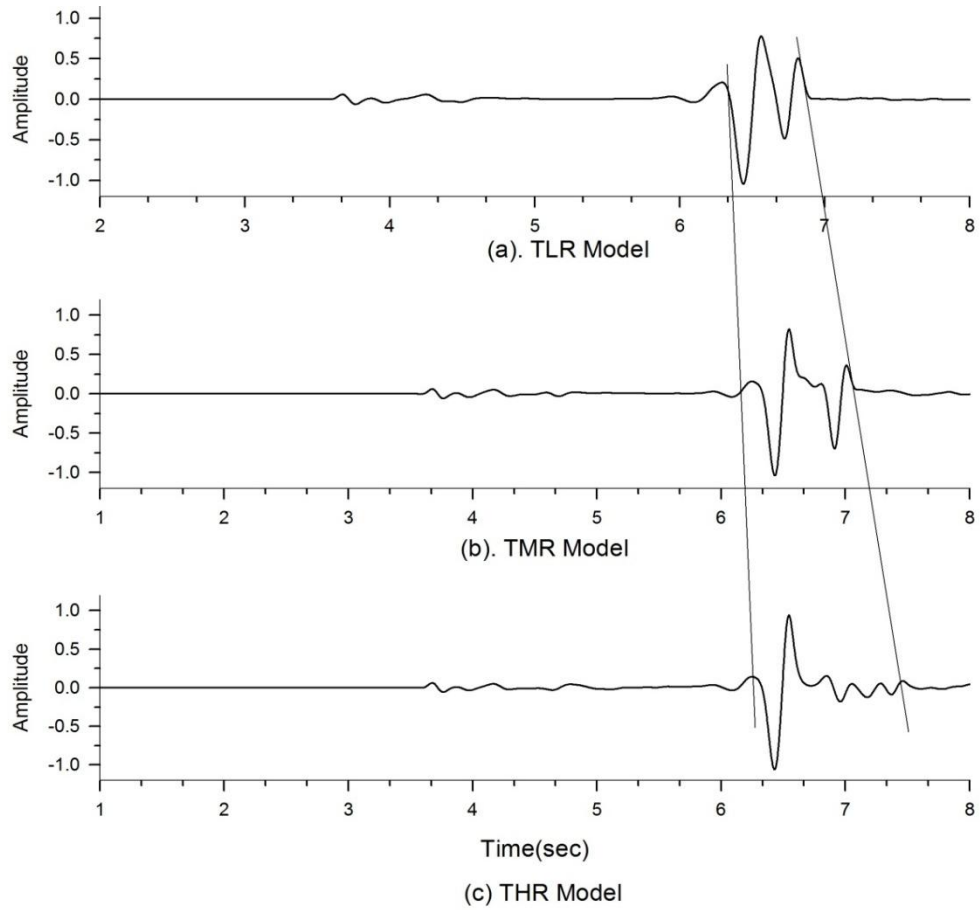

Figure 3.36 Time lag between arrival of splited Rayleigh waves after interaction with the ridge with shape ratio

To see the effect of shape ratio on the time separation of two Rayleigh waves, figure 3.36 was drawn for different shape-ratio. It appears that after the complex interaction with the topography, incident Rayleigh wave gets split into two part. The separation between the arrival of two waves increases with increase in shape ratio. First Rayleigh wave is arriving at the same time at the last station but there is a delay in arriving of second Rayleigh wave. We can inferred that first wave is passing almost unaffected by the topography and the second wave follows the along the flanks of the topography.

RAYLEIGH WAVERESPONSE OF VARIOUS COMBINATIONS OF RIDGE AND VALLEY TOPRGRAPHY

In order to quantify the effects of multiple ridge and valley topography on the characteristics of Rayleigh wave, we have taken two cases. In first case (A), when Rayleigh wave first interact with the ridge and in the second case (B) when Rayleigh wave first interact with the valley. Under acase 'A',we have taken six models as (a). TMRV Model as triangular-ridge-valley combination (b) TMRVR Model as triangular two-ridge and single-valley combination and (c) TM3RVR Model as triangular three ridge and three valley combinations. Similarly, for elliptical case as (a) EMRV Model, (b) EMRVR Model and (c) EM3RVR Model. In the same way in case 'B' also we have considered six models as (a) TMVR Model as triangular valley ridge combinations (b) TMVRV Model as triangular single ridge and two valley combinations and (c) TM3VRV Model as triangular three valley and three ridge combinations. Similarly for the elliptical case (a) EMVR Model, (b) EMVRV Model, (c) EM3VRVR Model. Ridge height is 360m and width 720m. Valley depth is 360m and width 720m.

The purpose of considering above two cases was to analyze that which combination is helping to dampen the effect of Rayleigh wave more and can later on suggest the construction of houses. We will also see that by what percentage energy in wave reduced after passing various combinations by analysis various spectral ratio and average spectral amplification graphs.

4.1 CASE "A": RAYLEIGH WAVE FIRST INTERACT WITH THE RIDGE

4.1.1 Triangular models

Figures 4.1 to 4.3 shows the TMRV, TMRVR and TM3RVR triangular ridge models, respectively in which ridge is first in the string.

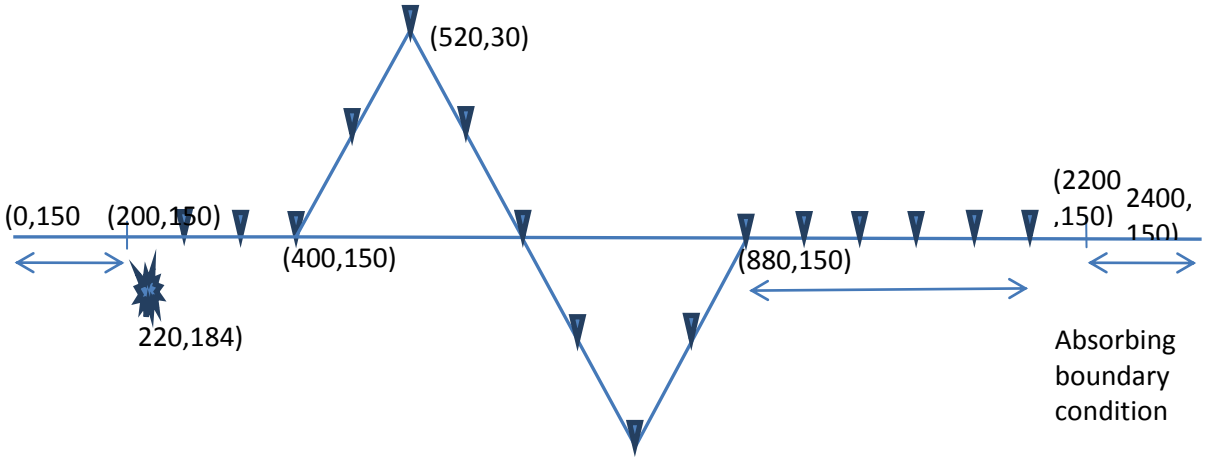

Fig. 4.1TMRV Model

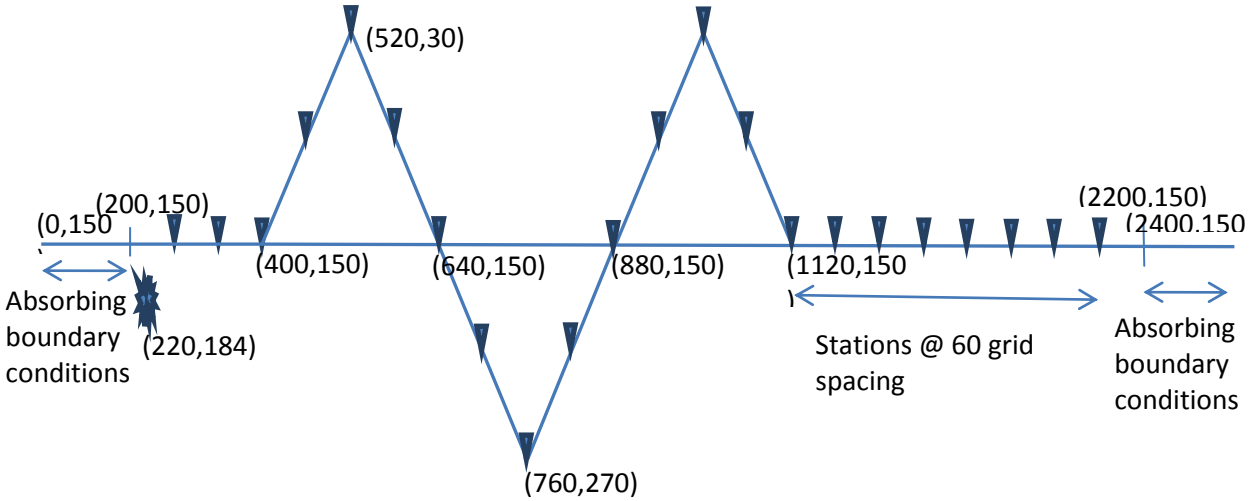

Fig 4.2 TMRVR Model

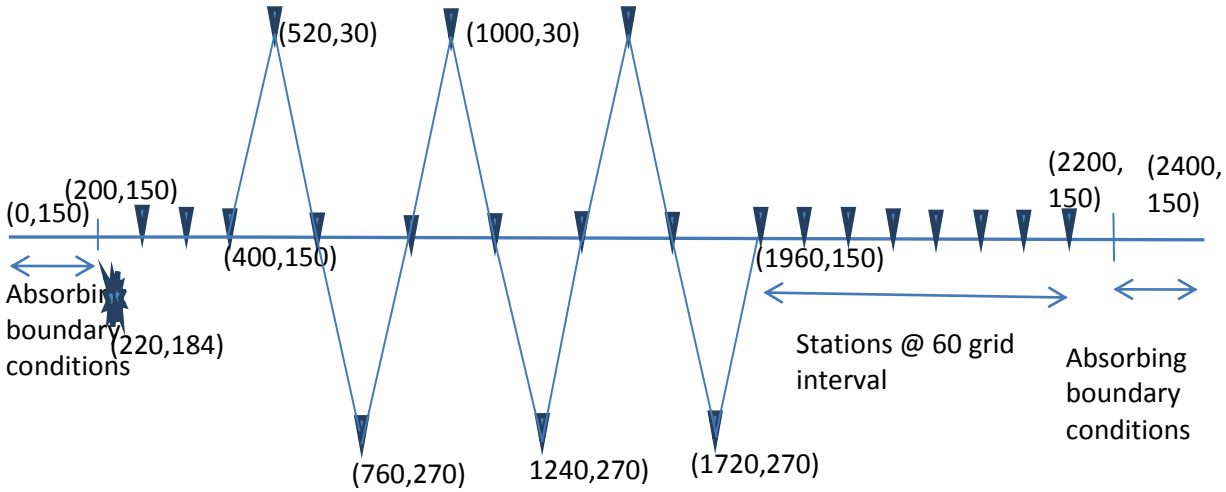

Fig. 4.3 TM3RVR Model

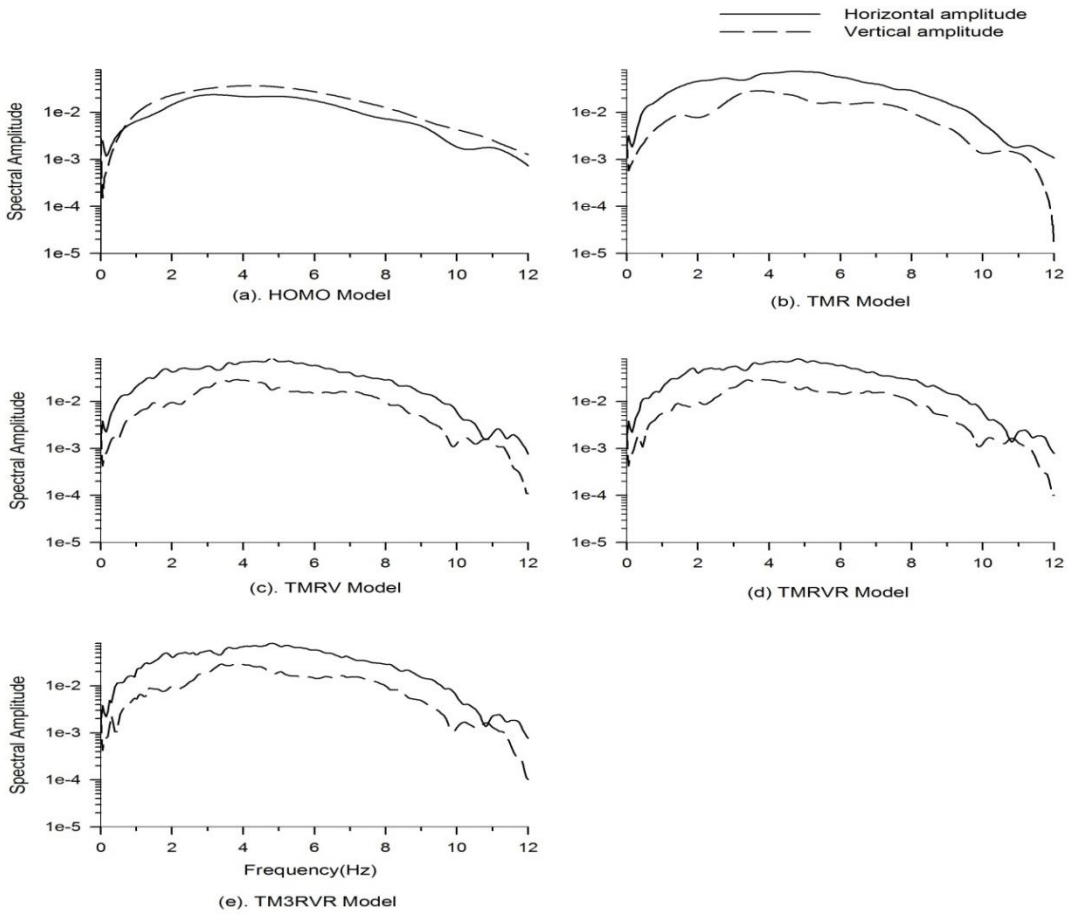

Fig 4.4 Spectral amplitude at the crest of first ridge in all models

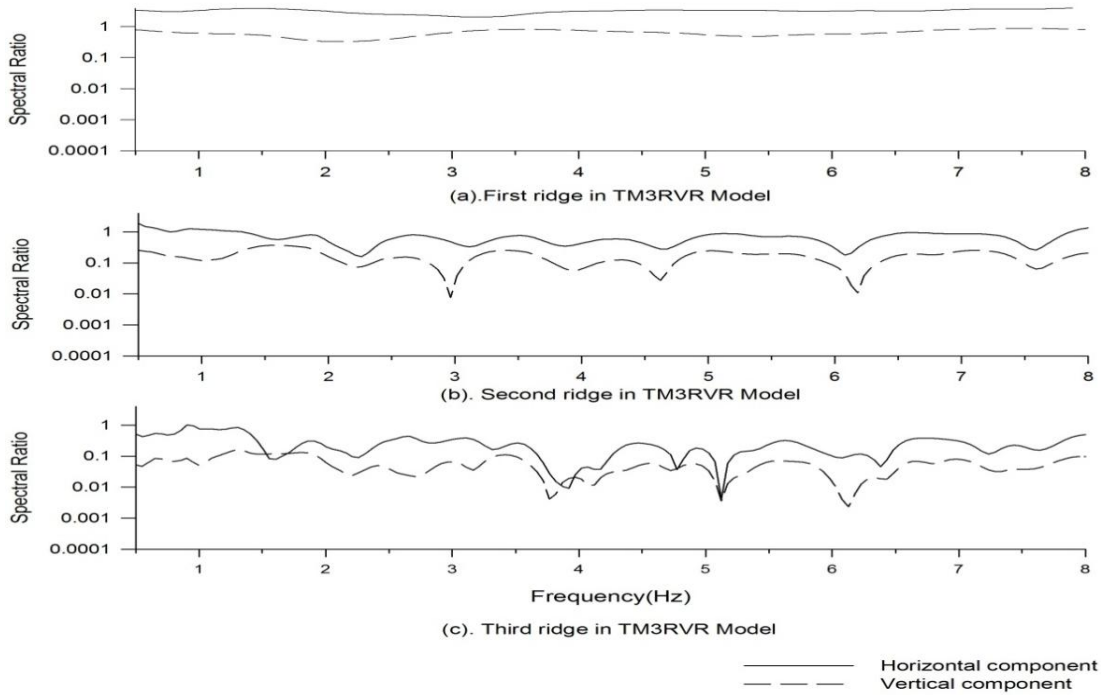

Fig 4.5 Spectral ratio at the crest of first, second and third ridge in all models when compared with the homogeneous model

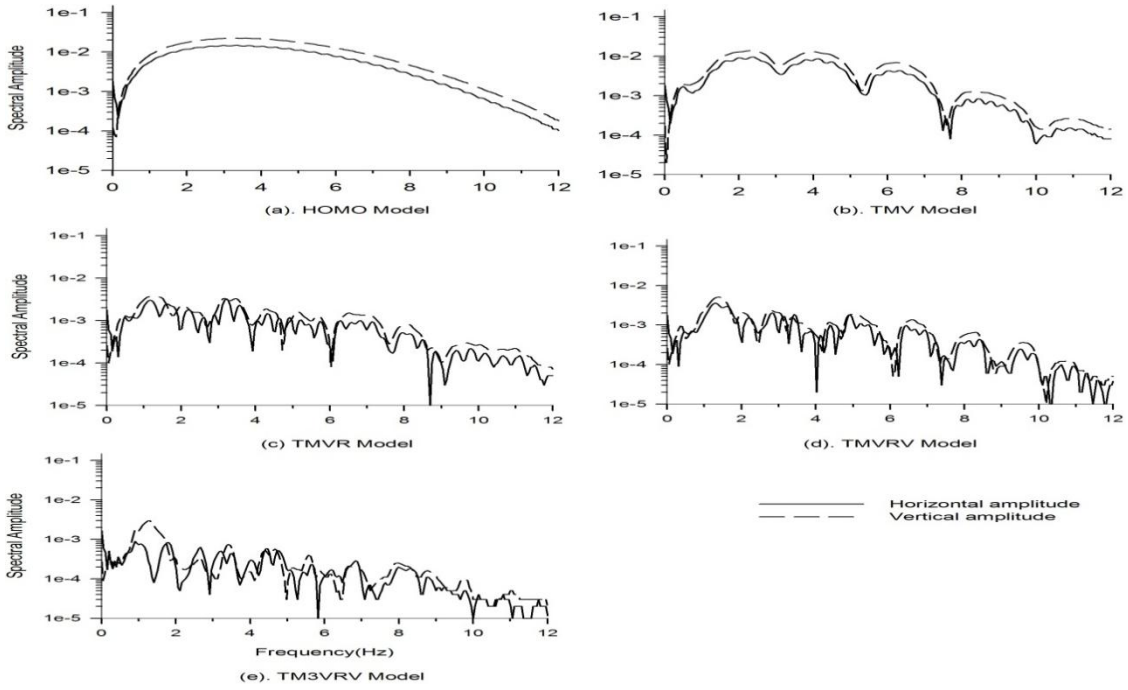

Fig 4.6 Spectral amplitude at the crest of first, second and third ridge in all models

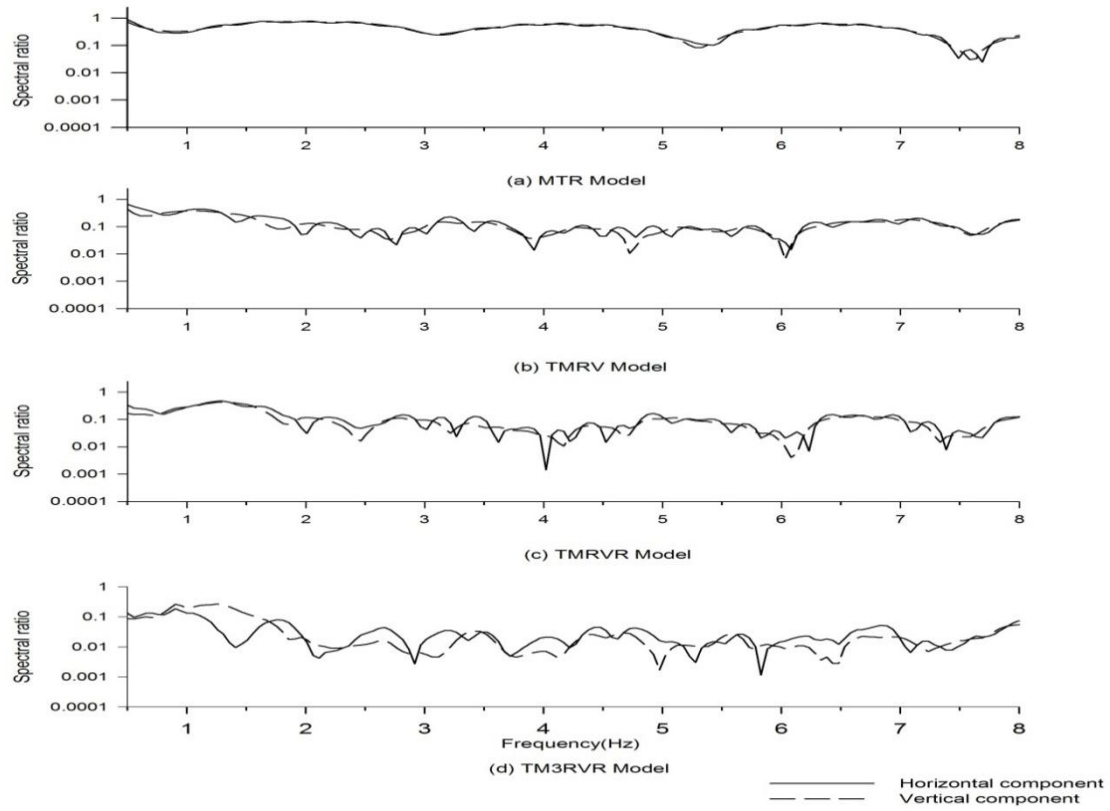

Fig 4.7 Spectral ratioat the last station in all models when compared with the homogeneous model

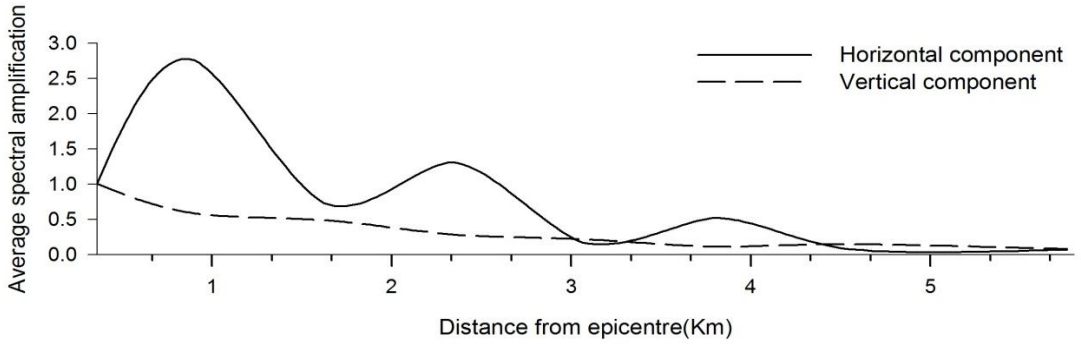

Fig.4.8 ASA of TM3RVR Model

Considering first ridge of all the models and computed response in terms of spectral amplitude as shown in fig 4.4. The response is nearly same at top of first ridge in all the models this may be due to the valley after the first ridge which is acting as a insulator to the reflected and diffracted Rayleigh wave.

On considering first, second and third ridge in model TM3RVR, horizontal component gets amplified at the crest of ridge in all the three ridge but this amplification goes on decreasing because of the valley in front of second and third ridge. Vertical component goes on decreasing because of de-amplification at every crest of ridge and bottom of valley. In case of models having ridge at the starting will amplify the horizontal component to a high value and hence it is disastrous to construct houses near this type of topography because wave contains energy even at longer distances.

4.1.2 Elliptical Model

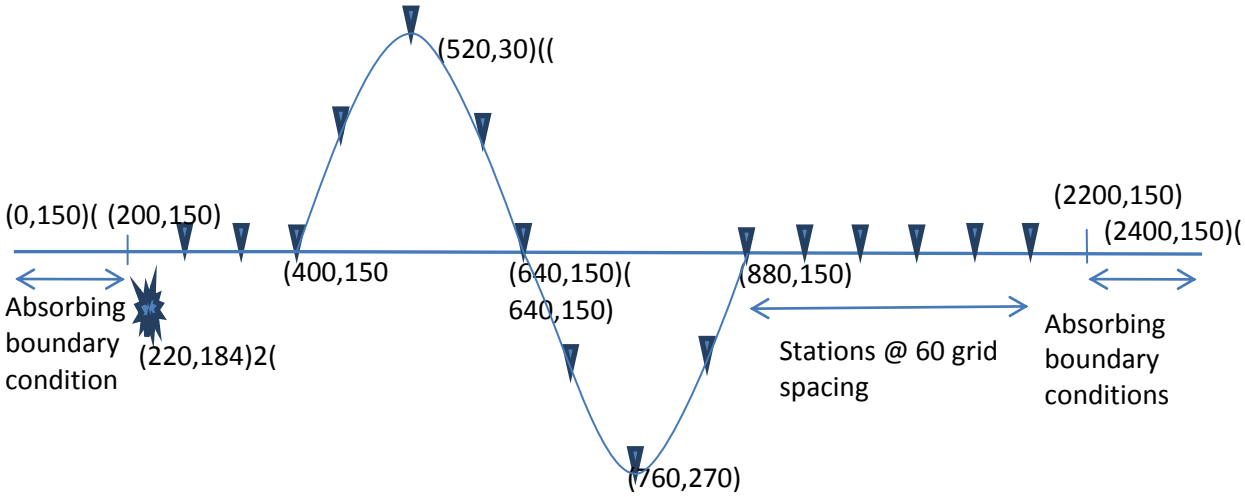

Fig 4.9 EMRV Model

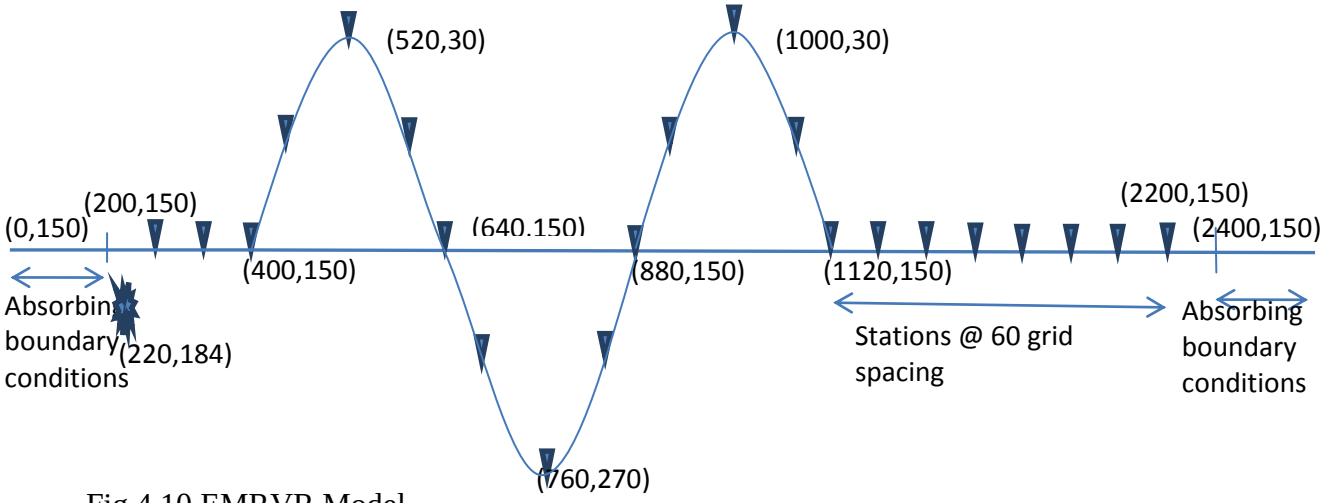

Fig 4.10 EMRVR Model

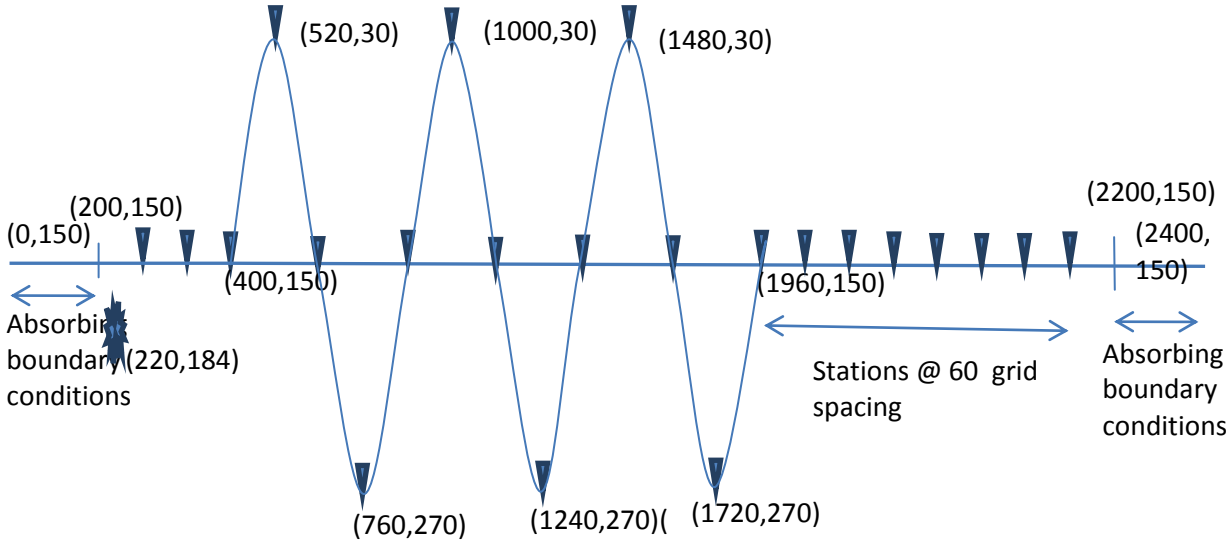

Fig 4.11 EM3RVR Model

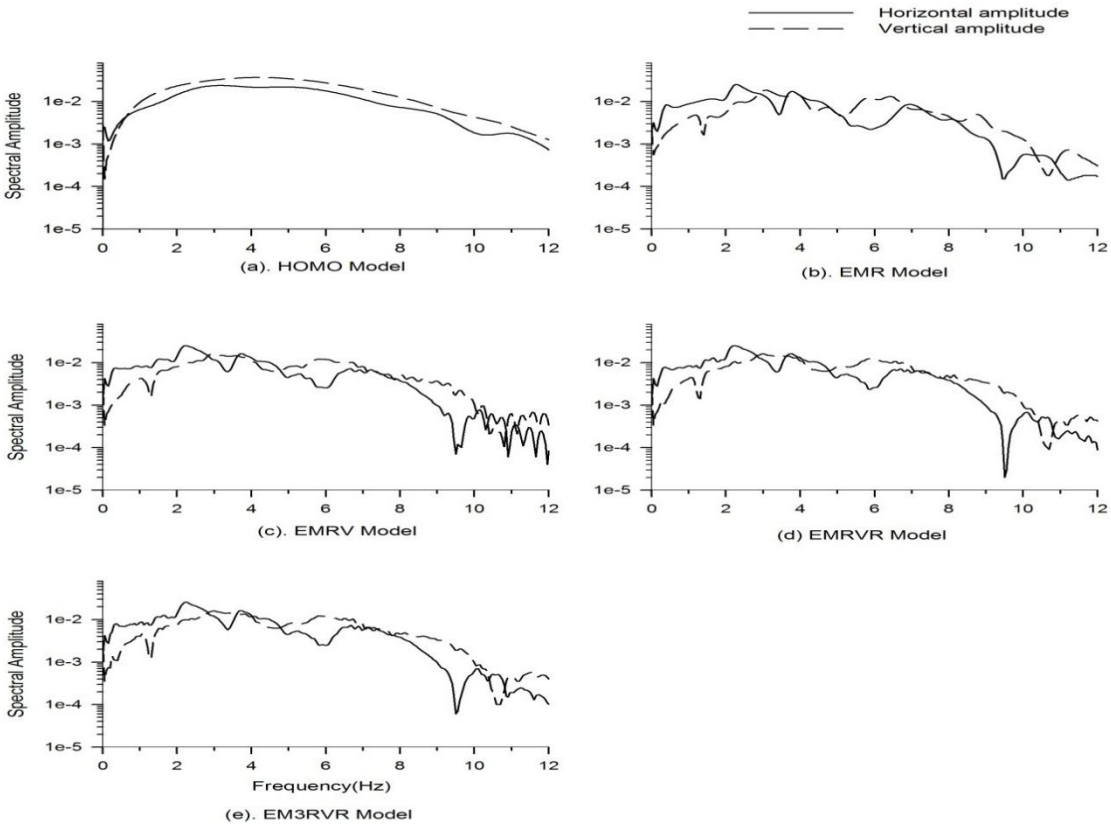

Fig 4.12 Spectral amplitude at the crest of first ridge in all models

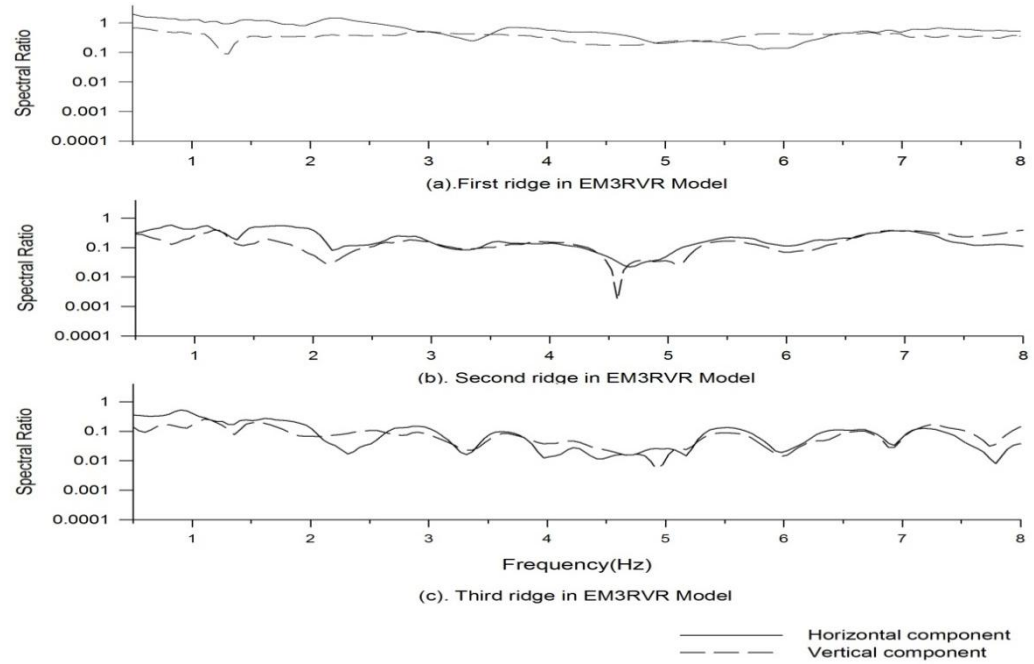

Fig 4.13 Spectral ratio at the crest of first, second and third ridge in all models when compared with the homogeneous model

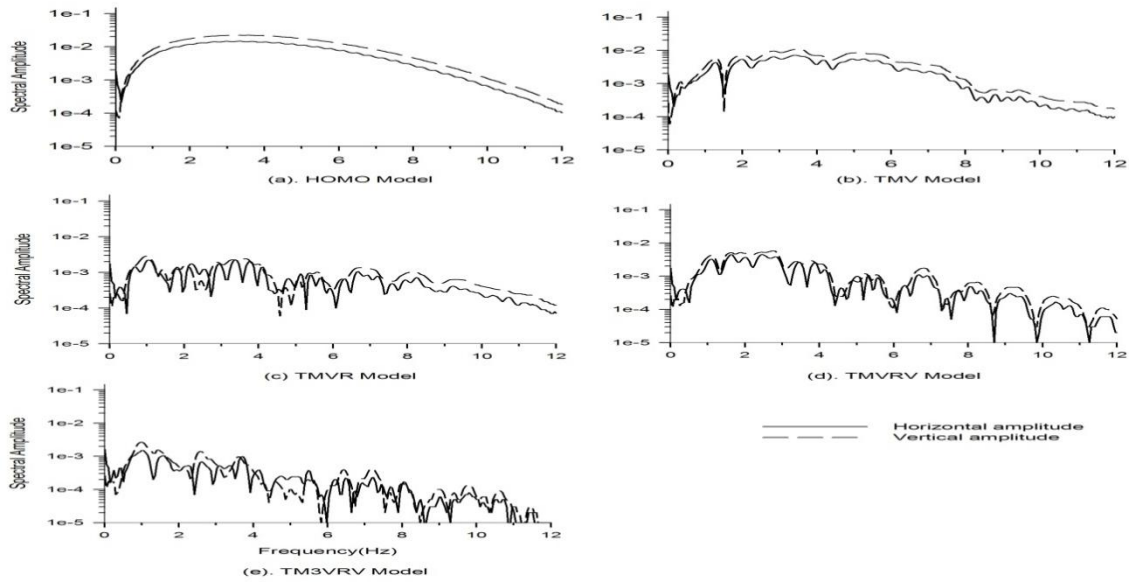

Fig 4.14 Spectral amplitude at the last station in all models when compared with the homogeneous model

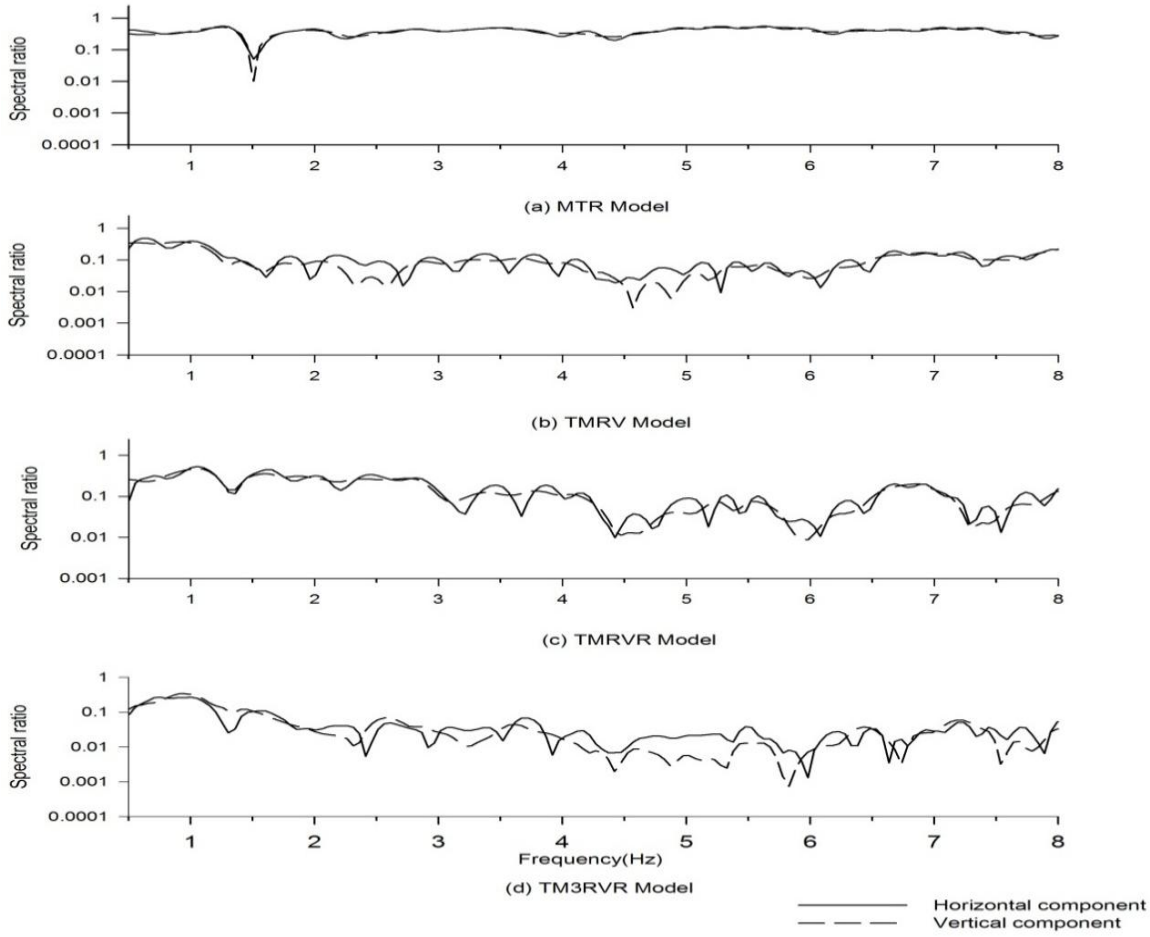

Fig 4.15 Spectral ratio at the last station in all models when compared with the homogeneous model

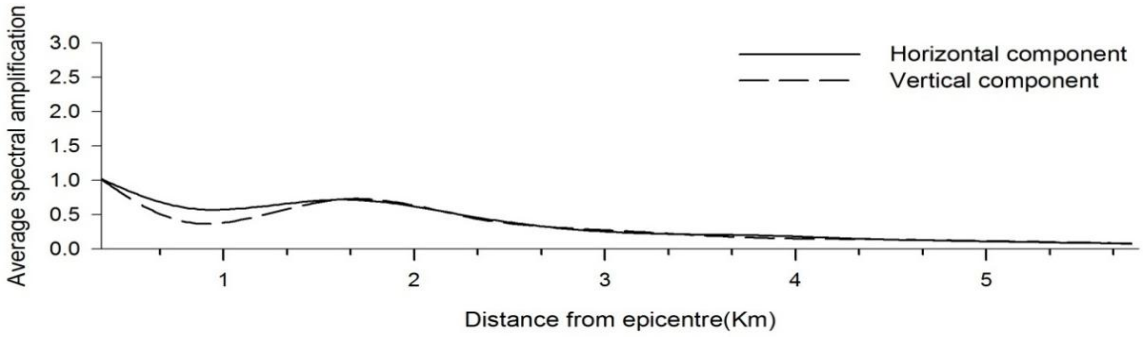

Fig 4.16 ASA of EM3RVR Model

Fig 4.12 shows the spectral amplitude of both horizontal and vertical component at the crest of first ridge in all elliptical models considered. The response due to first ridge is same in all the models. This may be due to the effects of valley just after the first ridge. Valley generally act as insulator which absorb all the diffracted and reflected waves and transmit only low energy signal.

Fig 4.14 and 4.15 shows the spectral amplification and spectral ratio at the last station. It is observed that as the number of ridge and valley combinations increases the rate of de-amplification also increases. Energy left with the signal at last station is very less in case of elliptical combination than triangular combinations.

Fig 4.16 shows the average spectral amplification at various stations. The amplification is less than 1 for both horizontal and vertical component means de-amplification goes on increases with increase in distance.

4.2 WHEN RAYLEIGH WAVE FIRST INTERACT WITH THE VALLEY

4.2.1 Triangular models

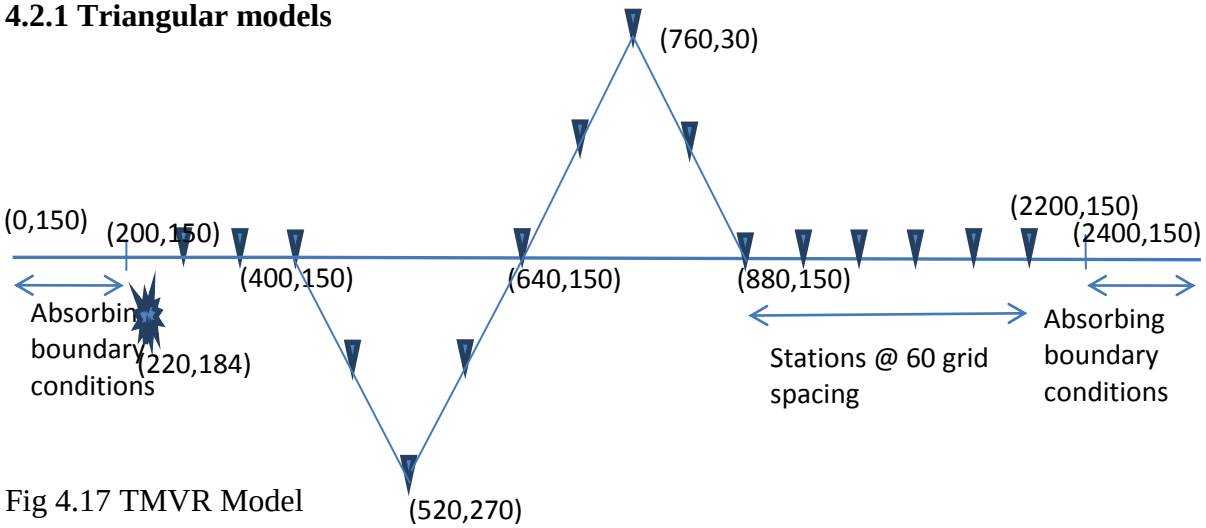

Fig 4.17 TMVR Model

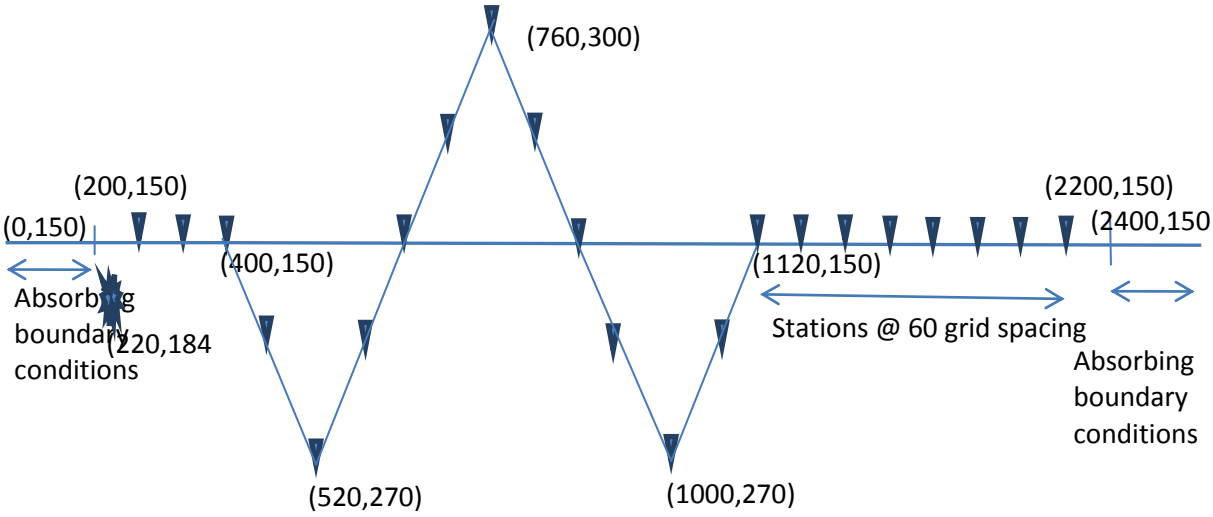

Fig 4.18 TMVRV Model

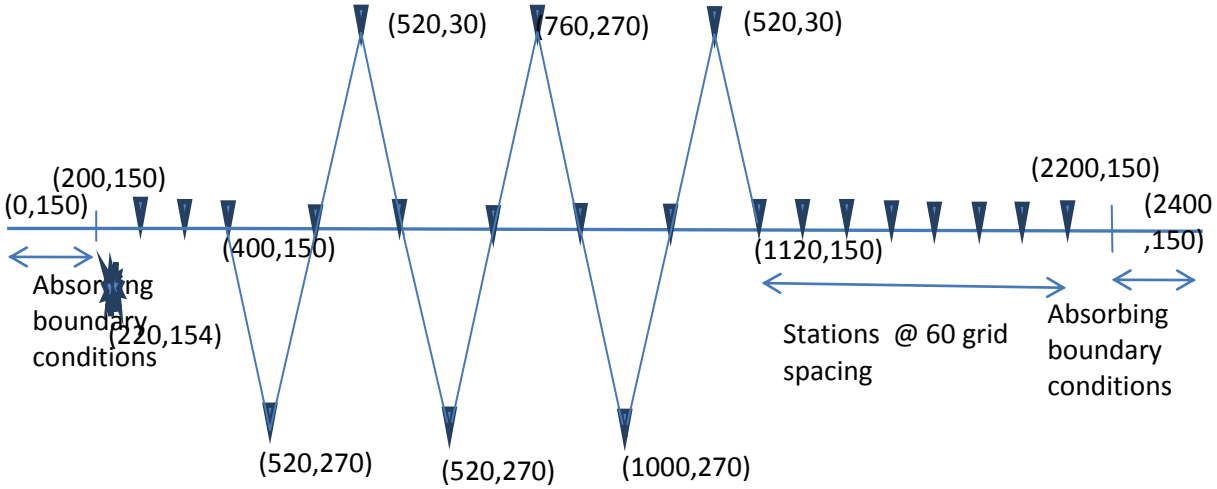

Fig 4.19 TM3VRV Model

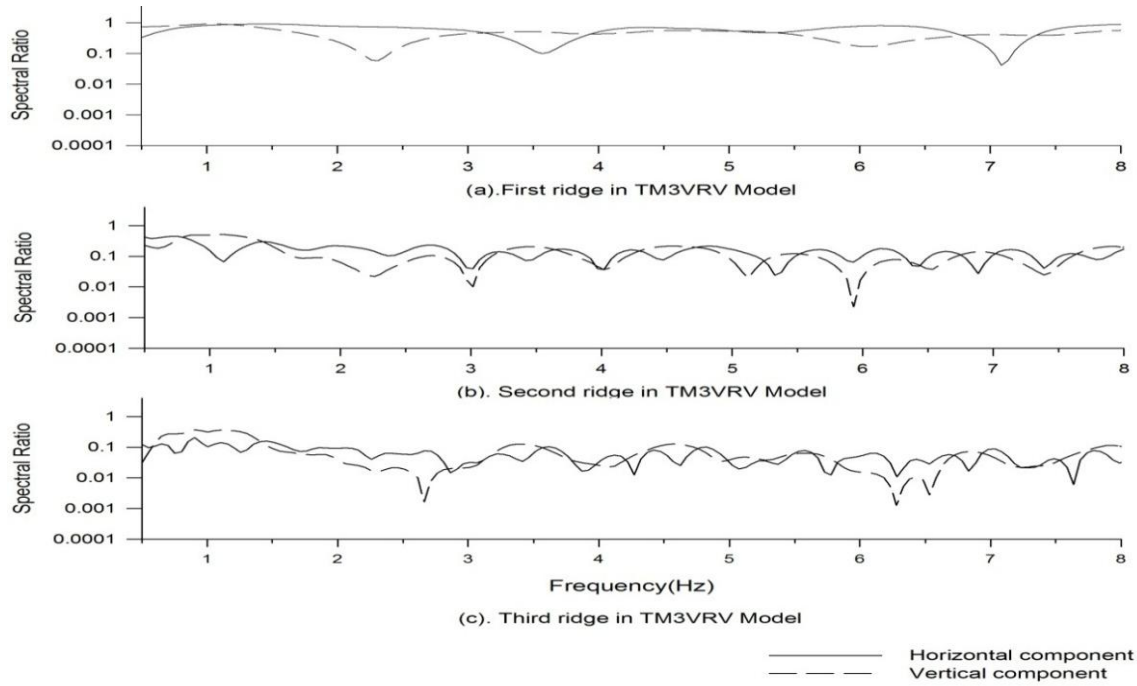

Fig 4.20 Spectral ratio at the bottom of first, second and third valley in all models when compared with the homogeneous model

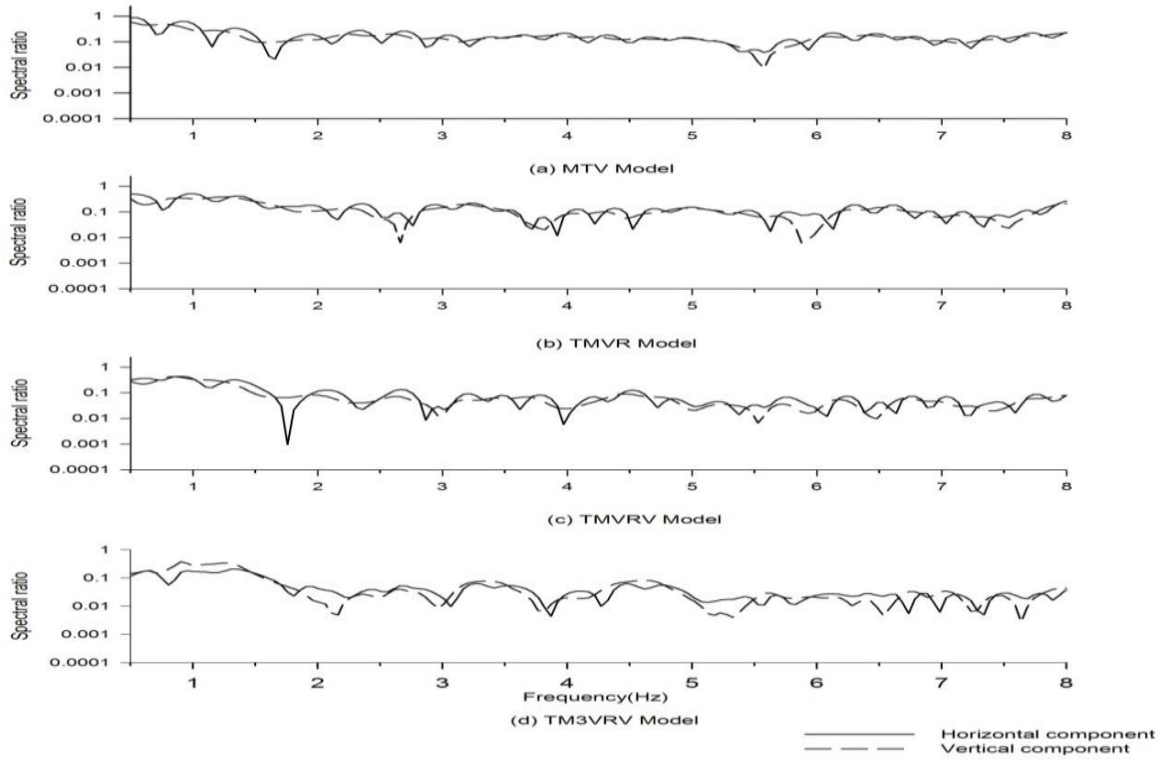

Fig 4.21 Spectral ratio at the last station in all models when compared with the homogeneous model

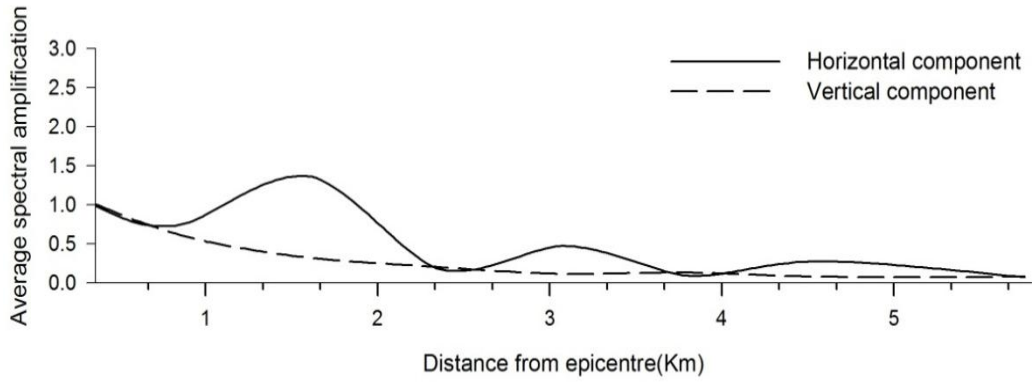

Fig 4.22 ASA of TM3VRV Model

In Fig. 4.20 we have computed the seismic response at first, second and third valley. The ratio is less than 1 in every case because valley de-amplify both the horizontal and vertical component. This ratio goes on decreasing as number of valley increases in the path of Rayleigh wave.

Fig 4.21 shows the spectral ratio at the last station in all models having valley at the starting of the combination. At the last stations in all the models the amplitude decrease to a significant amount hence more will be the combinations leads to more reduction in the amplitude of Rayleigh wave.

In case of Raleigh wave first interacting with the valley, amplitude of both horizontal and vertical component decreases first when encountered with first valley. But thereafter there is ridge which will amplify the horizontal component and again de-amplify the vertical component. This process repeats at every crest of ridge and bottom of valley. Therefore we see the various undulations in the horizontal component and continuous decrease in the vertical component in Fig 4.22.

4.2.2 Elliptical model

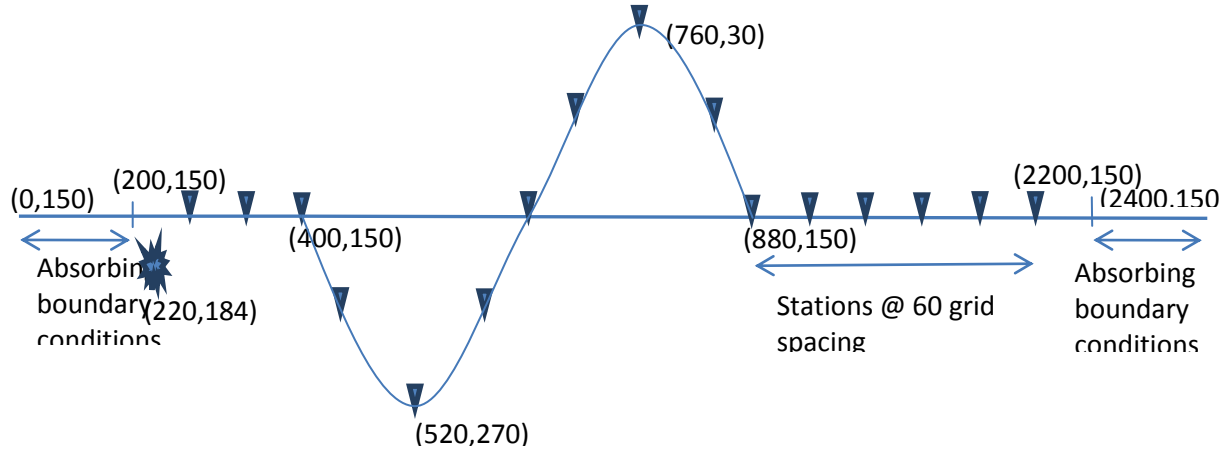

Fig 4.23 EMVR Model

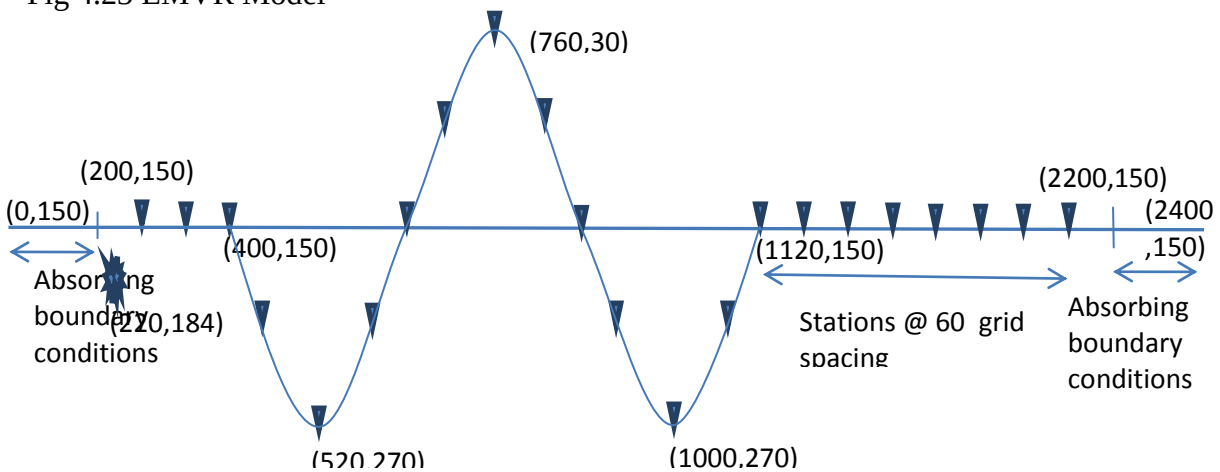

Fig 4.24 EMVRV Model

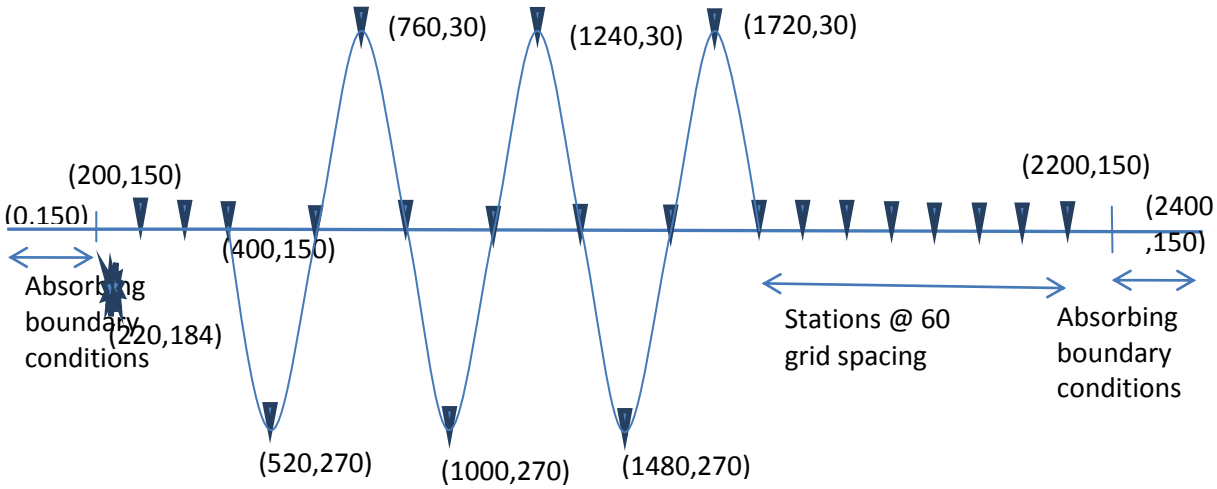

Fig 4.25 EM3VRV Model

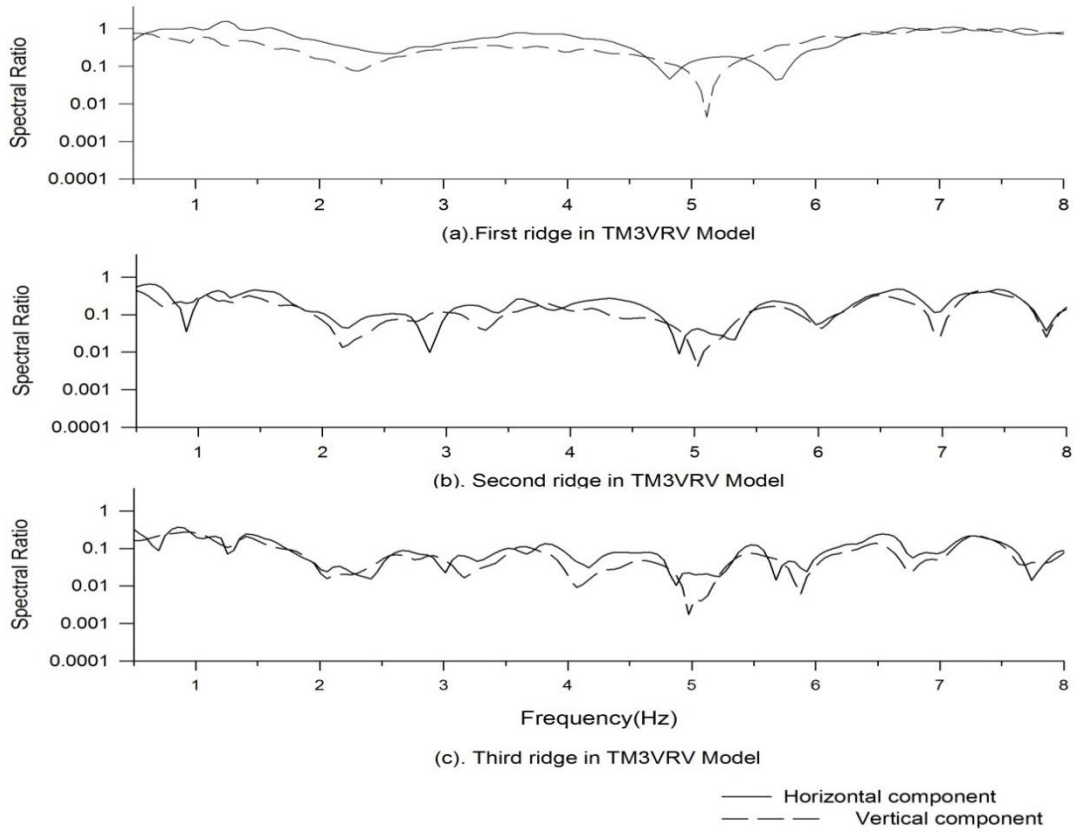

Fig 4.26 Spectral ratio at the bottom of first, second and third valley in all models when compared with the homogeneous model

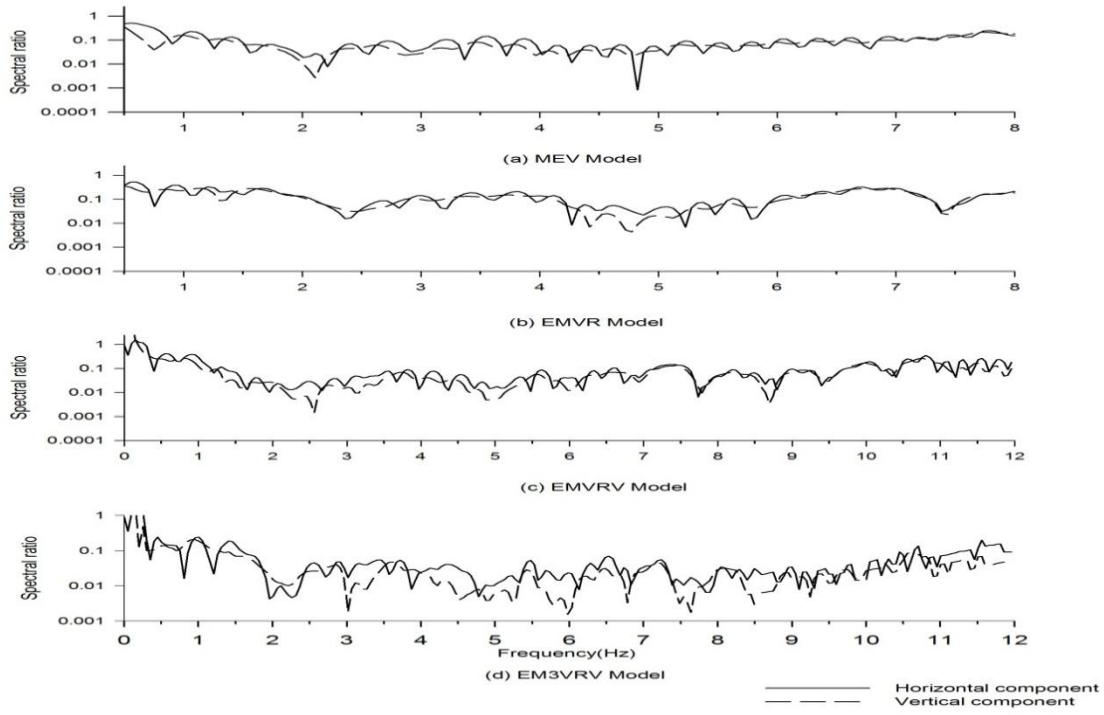

Fig 4.27 Spectral ratio at the last station in all models when compared with the homogeneous model

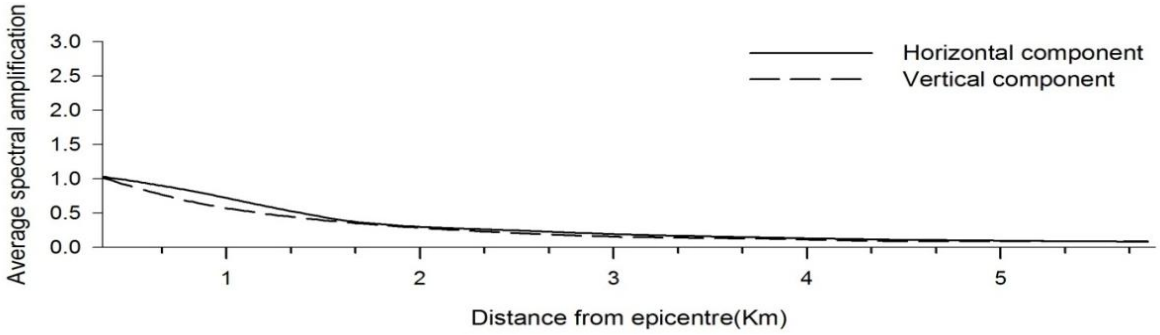

Fig 4.28 ASA of EM3VRV Model

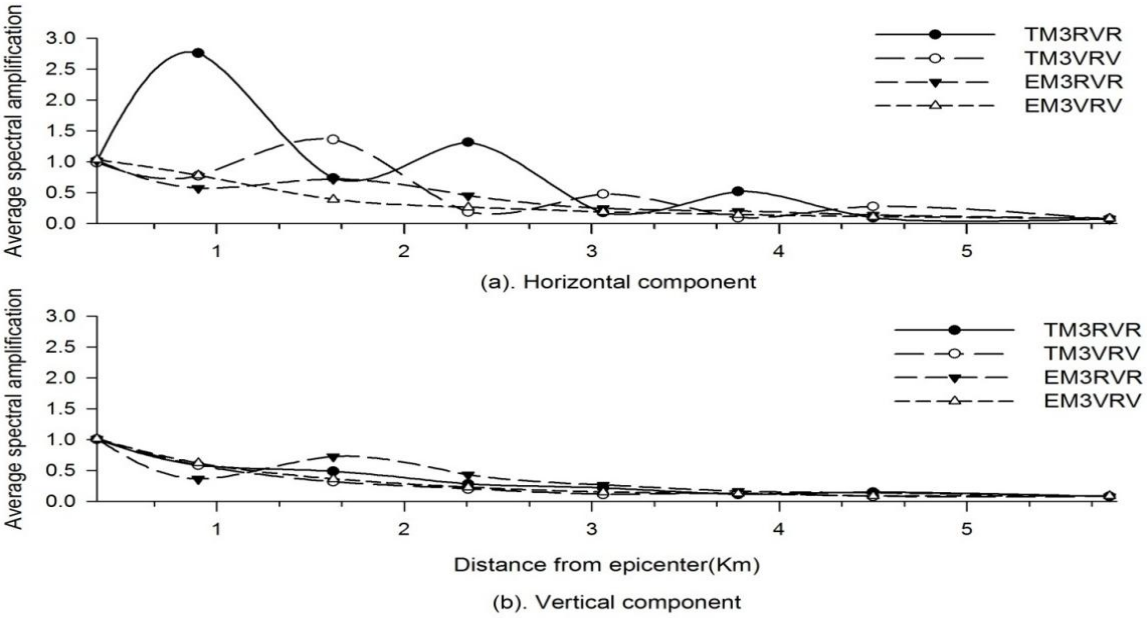

Fig 4.29 Comparing the ASA of various model combinations

In Fig 4.29 various ups and downs occurs in the horizontal component of Rayleigh wave. Ups are because of amplification of horizontal component at the crest of the ridge and downs are due to de-amplification at the bottom of the valley. Vertical component de-amplify at both the locations i.e. at crest of ridge and at bottom of valley but in case of elliptical model combinations there is some and fall. It is observed that energy remained in the signal is very less in case of elliptical valley ridge model combinations and triangular valley ridge model combinations.

DISCUSSION AND CONCLUSIONS

Till now mostly the effect of topography on body waves is analysed in details. A limited study has been done on surface waves. This dissertation is focused on the computation of effects of topography on Rayleigh wave characteristics using finite difference method. Various conclusions have been drawn from the analysis done over the different types of models.In homogeneous model decrease in amplitude of Rayleigh wave with distance occur due to damping effect. Generally the higher frequency waves are damped more.Analysis of simulated responses of the single triangular ridge model reveals that amplitude of the horizontal component of Rayleigh wave get maximum amplified and amplitude in vertical component gets de-amplified at the crest of ridge. The amplification in horizontal component and de-amplification in vertical component increases with increase in shape ratio. Hence Rayleigh wave gets horizontally polarized at crest of triangular ridge. As the shape ratio increases the amplitude of diffracted P-wave, S-wave and reflected Rayleigh wave also increases.

After the complex interaction with the topography Rayleigh wave splits into two waves and there is a time lag between the arrival of the two waves at a station. This lag increases with increase in shape ratio. It appears that the first arrival of Rayleigh is unaffected by the topography and the other wave travels through the flanks of topography which leads to the time lag.In case of triangular valley amplitude of both horizontal and vertical component decreases. Decrease in vertical component is more. This rate of decrease increases with increase in shape ratio. The spectra analysis at the last station in valley model reveals that energy in the Rayleigh wave is very less in high frequency range. So valley is generally acting as sinking zone where less reflection back of waves occurs. Hence we can recommend the construction in the nearby areas of valley where seismic risk is less as compared to the areas near to the ridge. Because horizontally polarized wave in case of ridge leads to chances of landslides, etc.

In case of elliptical ridge, horizontal component amplified but with a negligible amount and vertical component gets de-amplified. Further, there is no significant effect of shape ratio on Rayleigh wave characteristics in case of elliptical ridge. In case of elliptical valley both the horizontal and vertical components gets de-amplified and the rate of de-amplification increases with increase in shape ratio. Energy in the signal after passing the elliptical valley is lesser than in case of triangular valley.

The analysis of responses of a combinations of various ridge and valley topography together leads to a conclusion that if Rayleigh wave first interact with the valley in combination than high frequency will get absorbed and will pass the signal with very low energy content.Further, There is no significant variation in wave characteristics at the top of first ridge in the ridge valley train, This is because there is valley after every ridge which absorbs all diffracted and reflected wave. Generally elliptical valley is considered as best insulator for high frequency seismic waves than triangular valley.

REFERENCES

1. Boore D. M. (1972). A note on the effect of simple topography on seismic SH waves. Bull. Seism. Soc. Am.,62, 275-284.
2. Clayton, R. W. and Engquist, B. (1980): Absorbing side boundary conditions for wave equationmigration, Geophysics, 45, 895–904.
3. Francisco J. Sanchez –Sesma and Michel Campillo. 1991. Diffraction pf P,SV and Rayleigh wave by topographis features: a boundary integral formulation. Bulletin of the Seismological Society of Am~rica, Vol. 81, No. 6, pp. 2234-2253
4. Francisco J. Sanchez-Sesma a,b and Michel Campillo. 1993. Topographic effects for incident P, SV and Rayleigh waves. Instituto de /ngenier{a, UNAM Cd. Universitaria, Apdo. 70-472.
5. Fujii, K., S. Takeuchi, Y. Okano, and M. Nakano (1984). Rayleigh wave scattering at variouswedge corners, Bull Seism. Soc. Am. 74,41-60.
6. Narayan, J. P. and Rao, P. V. P. (2003): Two and half dimensional simulation of ridge effects onthe ground motion characteristics, Pure Appl. Geophys., 160, 1557–1571.
7. Pedersen, H., Hatzfeld, D., Campllo, M. and Bard, P. Y. (1994b): Ground motion amplitude acrossridges, *B. Seismol. Soc. Am.*, **84**, 1786–1800.
8. Sânchez-SesmaF,. J. and E. Rosenblueth (1979). Ground motion at canyons of arbitrary shapeunder incident SB waves, IntZ. J. Earthq. Eng. Struct. Dyn. 7,441-4450.
9. Sánchez-Sesma, F.J., Campillo, M., 1991. Diffraction of P, SV, and Rayleigh waves by topographicfeatures: a boundary integral formulation. Bull. Seismol. Soc. Am. 81,2234–2253.
10. Sánchez-Sesma, F. J. and Campillo, M. (1993): Topographic effects for incident P, SV and Rayleighwaves, Tectonophysics, 218, 113–125.
11. Shuo Ma*, Ralph J. Archuleta, and Morgan T. Page,2007. Effects of Large-Scale Surface Topography on Ground Motions,as Demonstrated by a Study of the San Gabriel Mountains,Los Angeles, California. Bulletin of the Seismological Society of America, Vol. 97, No. 6, pp. 2066–2079
12. Trifunac, M. D. (1971). Surface motion of a semi-cylindrical alluvial valley for incident plane SH waves, Bull. Seism. Soc. Am. 61, 1755-1770.

13. Trifunac, M. D. (1973), Scattering of plane SH waves by a semi-cylindrical canyon, IntZ. J.Earthquake Eng. Struct. Dyn. 1,267-281.
14. Wang, L., Luo, Y., Xu, Y., 2012. Numerical investigation of Rayleigh-wave propagation ontopography surface. J. Appl. Geophys. 86, 88–97.
15. Wong, H.L., 1982. Effect of surface topography on the diffraction of P, SV, and Rayleighwaves. Bull. Seismol. Soc. Am. 72 (4), 1167–1183.
16. Zhang, L. and Chopra, A.K., 1991. Three-dimensional analysis of spatially varying ground motions around a uniformcanyon in a homogeneous half-space. Int. J. Earthquake Eng. Struct. Dyn., 7: 441-450. Eng. Struct. Dyn., 20: 911-926.
17. Zhou, H., Chen, X., 2007. A study on the effect of depressed topography on Rayleigh surfacewave. Chin. J. Geophys. 50 (4), 1018–1025.
18. Zeng, C., Xia, J., Miller, R.D., Tsoflias, G.P., 2012a. An improved vacuum formulation for 2Dfinite-differencemodeling of Rayleigh waves including surface topography and internaldiscontinuities. Geophysics 77 (1), 1–9.